CALIFORNIA INSTITUTE OF TECHNOLOGY

EARTHQUAKE ENGINEERING RESEARCH LABORATORY

MODE SUPERPOSITION METHODS APPLIED TO LINEAR MECHANICAL SYSTEMS UNDER EARTHQUAKE TYPE EXCITATION

by

Howard C. Merchant

Pasadena, California

March 1961

MODE SUPERPOSITION METHODS APPLIED TO LINEAR MECHANICAL SYSTEMS UNDER EARTHQUAKE TYPE EXCITATION

Thesis by

Howard Carl Merchant

In Partial Fulfillment of the Requirements
For the Degree of
Doctor of Philosophy

California Institute of Technology
Pasadena, California
1961

ACKNOWLEDGEMENT

The author wishes to express his appreciation to Dr. D. E. Hudson, Dr. T. K. Caughey and Dr. G. W. Housner for their many helpful suggestions during the course of this work and to the National Science Foundation for granting fellowships under which part of this work was completed.

ABSTRACT

The determination of the maximum dynamic responses of a multidegree of freedom mechanical system under earthquake type excitation using mode superposition methods is the general problem considered. The experimental work was carried out using a special purpose electronic differential analyzer involving a three degree of freedom system, or a three mode approximation to a larger system.

The results indicate that a suitably weighted average of the sum of the absolute values and the square root of the sum of the squares of the individual mode contributions gives a practical design criterion for the base shear forces. For critical designs this weighted average reduces to the absolute sum of the modes, which will be close to the true value for a significantly high percentage of the cases. The base moment may be more accurately approximated than the base shear by use of the first mode alone.

TABLE OF CONTENTS

LIST OF FIGURES

LIST OF TABLES

NOTATION

$a, b, \bar{a}, \bar{b}$	Constants
c_i	Viscous damping coefficients
$E(\xi)$	Expected value of ξ
f	Frequency (cycles/sec)
g_i	Generalized force
G_i	Generalized force coefficient ($G_i\ddot{y} = g_i$)
h_i	Height of ith floor above base
i	$\sqrt{-1}$
k_i	Spring constant (shear) of spring below ith mass
K_i	$\dfrac{\omega_i^2}{k/m}$
ℓ	Height in lines of a trace on oscilloscope
M_B	Base moment
m_i	Mass
n	Constant, generally number of degrees of freedom
q	Constant
r	Height in g's of an accelerogram trace
R	Response
t, t_r	Time (true)
t_a	Time (analog)
T	Natural period (sec)
V_B	Base shear
x_{ai}	Oscilloscope reading of analog combination (lines)
x_i	Relative coordinate (real system)
$\overline{x_i}$	Absolute coordinate

$(\dot{\ })$	First derivative with respect to time
$(\ddot{\ })$	Second derivative with respect to time
y	Base motion ($\ddot{y}(t)$ assumed equal to earthquake accelerogram)
α, β	Constants
ξ_{ai}	Oscilloscope reading of analog results (lines)
ξ_i	Normal coordinates
ξ_{si}	Mode response to $\ddot{y}(t)$ (maximum is spectrum point)
$\overline{\xi_{si}}$	Absolute ξ_{si}
ρ	Critical damping ratio ($c/c_c = c/2\sqrt{km}$)
σ	Variance
$\sum_i$	Summation on i
ω, ω_r	Circular frequency (true, radians/sec)
ω_a	Circular frequency (analog)
$\{\ \}$	Column matrix
$[\ ]$	Square matrix
$[\ ]^T$	Transpose of matrix $[\ ]$
$[I]$	Identity matrix
$\{\phi^i\}$	Mode shape of ith mode
$[M]$	Mass matrix
$[C]$	Damping matrix
$[K]$	Spring matrix

I. INTRODUCTION

An important vibration problem that is frequently encountered in many different engineering applications is the transient response of multidegree of freedom systems. The excitation of buildings by earthquakes is an example of such a problem. The excitation of a structure or machine by a bomb-shock, or of a submarine by explosive-generated water pressures are other examples. The characteristic features of all of these problems are that the vibrating system has a large number of degrees of freedom and that the exciting force has no simple description. In fact, in most cases it is not possible to predict the exciting force that might act on the structure other than in a probabilistic fashion.

In every actual vibration problem there are, of course, a great number of degrees of freedom, but it is customary to rule out most of these on the basis that they have no significant influence on the problem to be investigated. For the type of problem described in the preceding paragraph, the physical system and the exciting force are such that a relatively large number of degrees of freedom cannot be eliminated on the basis of inspection. The question then becomes one of determining the degrees of freedom that must be retained in the analysis. The answer to this question will, of course, be dependent upon the nature of the physical system and the characteristics of the exciting force. The essential problem is how to determine the maximum response in the sense of maximum displacement, maximum strain, maximum strain energy, etc., to a degree of precision satisfactory for engineering purposes.

In principle, a theoretical analysis would answer all of these questions. For example, in the case of a linear system acted upon by a force that is a random function of the stationary Gaussian type, it is possible, on the basis of a theoretical analysis, to make statements in a probabilistic sense about certain average values of system response. If such an analysis could be extended to transient, non-Gaussian excitations to the extent that meaningful statements could be made about maximum displacement, maximum stress, etc., the problem would be solved. The difficulties of such an analysis preclude its use and experimental or computational methods must be employed.

One approach to the problem would be to obtain a complete time solution by a graphical or numerical method. This, of course, would give the desired results for specific cases but because of the complicated inputs and structural configurations, the time required for any general studies would be prohibitive. Another approach would be to turn to analog or digital computer methods.

Mechanical analogs in the form of models on shaking platforms could be used, but this would be a laborious procedure since the structural parameters could not be easily altered to handle different problems. A mechanical analog in the form of a torsion pendulum has been used, particularly for single degree of freedom systems (1).

Direct electrical analog circuits are also a possibility. The versatility and speed of the electric analog is far superior to a mechanical analog (2, 3). Electric analog inputs are in the form of electrical signals obtained from such devices as photoelectric readers, magnetic tapes, etc. (4). With the same type of input there is also the possibility of using a differential analyzer with active electrical elements, to carry out the mathematical steps given by the equations of motion of the mechanical system.

Solution of the equations of motion by numerical integration has become feasible with the advent of high speed digital computers (5, 6, 7, 8). The inputs must be converted to a digital numerical form which may be a major time consuming step in the calculation.

With any of the above computation methods the complete time response of the system may be obtained by two different approaches. With one approach the response may be determined by treating the entire system as one complicated problem. The other method involves using modal techniques by means of which the single large system may be broken down into a number of smaller ones and each considered as a separate relatively simple problem.

The solution of the single large problem has the defect of lack of generality and does not directly indicate possible design procedure. The modal approach offers hope of more general conclusions and a simplified approximate design procedure.

For linear systems with small damping, or damping of a special type, modal analysis is applicable. An n degree of freedom system may be broken down into n single degree of freedom systems by this method. The single degree of freedom time responses modified by the proper mode participation factors are combined to give the time response of the complete system. This can be accomplished in mechanical analog computation using a torsion pendulum, the mode responses being combined graphically (9). A set of torsion pendulums can also be used to represent a multidegree of freedom system, the mode responses being combined electrically (10). It is also possible to set up modes on either the passive analog type computer or the electronic differential analyzer. A differential analyzer analog type computer using the modal technique was employed to collect the data for this thesis.

Even the modal approach may be rather complicated for actual structures and hence some further simplification would be desirable. Since the maximum response only, rather than the complete time response, is ordinarily needed to determine design requirements, the maximum response becomes the quantity of interest in most cases. This reduces the required data from a response versus time curve to a single maximum point.

With a combination of modal methods and a maximum value limitation, one is able to make a more general statement about the solution. One way of doing this is by introducing the concept of the response spectrum (11). The response spectrum curve for a particular input is defined as the maximum response occurring in a single degree of freedom system, plotted versus the undamped natural period of the system. A family of curves is obtained by varying the damping. The usual spectrum is a relative velocity curve, but relative displacement and absolute acceleration spectra are also used. Note that the response spectrum alone does not constitute a complete description of system response since all phase information has been lost.

Spectra may be obtained using a torsion pendulum mechanical analog (11, 12). A special purpose passive electrical analog has been developed which allows more rapid evaluation of earthquake spectra (4). Spectra points may also be obtained directly from a reed gauge which is essentially a group of single degree of freedom mechanical systems with a provision for recording extreme values (13).

Attempts to define spectra for a system of more than one degree of freedom have not met with success because of the large number of parameters involved.

The use of the single degree of freedom spectrum data when a particular multidegree of freedom system is to be considered proceeds through the following steps:

1. Calculate or experimentally obtain the normal modes for the system. The quantities needed are the frequencies, mode shapes and damping for the n modes.
2. For each mode, obtain from the spectrum curve for the given input, the maximum response for the appropriate damping and period as calculated in step 1.
3. Alter each spectrum value by the appropriate participation factor calculated from the data of step 1 to obtain the contribution to the total response of the complete system from each mode.
4. Combine the values of the individual mode contributions from step 3 to find the total response.

Once the spectra have been obtained and the first three steps listed above have been carried out, the question becomes one of determining the proper method of combination of modal responses. For an n degree of freedom system there will be n values to combine with no knowledge of the phase or time relationship. In certain instances, however, multidegree of freedom systems behave essentially as single degree of freedom systems and no combination problems arise. For example, the base moment in a structure undergoing earthquakelike excitation may be obtained approximately by considering only the first mode.

The sum of the absolute values of each modal contribution gives an upper bound to the total system response (14). Since this would in general be expected to be overly conservative, a closer approximation to the actual response would be desirable for design considerations. One approach which has been suggested is to add a fixed percentage of the higher modes to the first mode or to increase the first mode by a fixed percentage. This has been investigated by Clough (15) using digital techniques and actual earthquake inputs. It has been shown that under certain conditions for a single pulse type shock, the algebraic sum gives a more accurate representation of the true maximum response (16). Based on statistical considerations, the square root of the sum of squares of the mode contributions has also been postulated (17, 18, 19). The average of the responses obtained using the absolute values of the mode contributions and the square root of the sum of the squares has also been suggested as an empirical rule. This suggestion has been based on data obtained by making calculations on a particular structure under a specified earthquake excitation (7).

The above methods may give widely varying results. Part of what follows is concerned with verifying the applicability, if at all, of the different methods and the range where they may be used.

II. GENERAL EQUATIONS

The model used is based on the following assumptions:

1. Concentrated masses at the floor levels connected by a system of weightless springs and damping elements.
2. Linear spring forces.
3. Classical normal modes exist unless otherwise specified.
4. No base compliance.
5. Deformation in shear only, the floor structure assumed to undergo no rotation and to be assumed infinitely rigid.

Refer to (fig. 1).

The general method of modal analysis for such a model is well known (5,20). A brief outline of the method is presented here to provide a basis for understanding the experimental approach of this thesis and to indicate how the cases investigated were chosen in order that they have meaning in an engineering situation.

The equations of motion for the undamped case take the form

$$\left[M\right]\left\{\ddot{x}\right\} + \left[K\right]\left\{x\right\} = \left[M\right]\left\{-\ddot{y}\right\} \tag{1}$$

or for the homogeneous case

$$\left[M\right]\left\{\ddot{x}\right\} + \left[K\right]\left\{x\right\} = 0 \tag{1a}$$

where

$$[M] = \begin{bmatrix} m_1 & 0 & \cdots & 0 \\ 0 & m_2 & & \vdots \\ \vdots & & \ddots & \\ 0 & \cdots & & m_n \end{bmatrix}$$

$$[K] = \begin{bmatrix} k_1 & -k_1 & 0 & \cdots & 0 \\ -k_1 & k_1+k_2 & -k_2 & & \vdots \\ 0 & -k_2 & \ddots & & \\ & & & & -k_{n-1} \\ 0 & \cdots & & -k_{n-1} & k_{n-1}+k_n \end{bmatrix}$$

$$\{\ddot{x}\} = \begin{Bmatrix} \ddot{x}_1 \\ \ddot{x}_2 \\ \vdots \\ \ddot{x}_n \end{Bmatrix} \qquad \{x\} = \begin{Bmatrix} x_1 \\ x_2 \\ \vdots \\ x_n \end{Bmatrix} \qquad \{-\ddot{y}\} = \begin{Bmatrix} -\ddot{y} \\ -\ddot{y} \\ \vdots \\ -\ddot{y} \end{Bmatrix}$$

The homogeneous solution for the above takes the form

$$\{x\} = q\, e^{i\omega t}\{\phi\}$$

where q is a scaler

$\{\phi\}$ a dimensionless vector

t is time

ω a scaler

Upon introducing equation 2, equation 1a becomes

$$q e^{i\omega t} \left\{ [K] \{\phi\} - \omega^2 [M] \{\phi\} \right\} = 0 \tag{3}$$

$$\left[[M]^{-1} [K] - \omega^2 [I] \right] \{\phi\} = 0 \tag{3a}$$

For equation 3a to possess a solution the following determinate must vanish:

$$\begin{vmatrix} \frac{k_1}{m_1} - \omega^2 & \frac{-k_1}{m_1} & 0 & \cdots & 0 \\ \frac{-k_1}{m_2} & \frac{k_1+k_2}{m_2} - \omega^2 & \frac{-k_2}{m_2} & & \vdots \\ 0 & \frac{-k_2}{m_3} & \ddots & \ddots & \frac{k_{n-1}}{m_{n-1}} \\ \vdots & & & & \\ 0 & \cdots & \frac{k_{n-1}}{m_n} & \frac{k_{n-1}+k_n}{m_n} & -\omega^2 \end{vmatrix} = 0 \tag{4}$$

This is the frequency equation. For each frequency (ω_i) there corresponds a mode shape ($\{\phi^i\}$) defined to within a constant as given by equation 3a.

The $\{\phi^i\}$ may also be expressed as the cofactors of any row of the determinate 4. An example for a three degree of freedom system using the cofactors of row two, would be:

$$\left\{\phi^i\right\} = \left\{\begin{matrix} -\left(-\frac{k_1}{m_1}\right)\left(\frac{k_2+k_3}{m_3}-\omega_i^2\right) \\ \\ \left(\frac{k_1}{m_1}-\omega_i^2\right)\left(\frac{k_2+k_3}{m_3}-\omega_i^2\right) \\ \\ -\left(\frac{k_1}{m_1}-\omega_i^2\right)\left(-\frac{k_2}{m_3}\right) \end{matrix}\right\} \qquad (5)$$

Using equation 3a the following conditions may be established,

$$\begin{aligned} \left\{\phi^k\right\}^T [M] \left\{\phi^j\right\} &= 0 \qquad j \neq k \\ \left\{\phi^k\right\}^T [K] \left\{\phi^j\right\} &= 0 \qquad j \neq k \end{aligned} \qquad (6)$$

repeated roots excluded. The superscript T indicates a transposed matrix. Let

$$[Q] = \left[\phi^1 \; \phi^2 \; --- \; \phi^n\right] \qquad (7)$$

$$\{x\} = [Q] \; \{\xi\} \qquad (8)$$

where

$$\{\xi\} = \left\{\begin{matrix} \xi_1(t) \\ \xi_2(t) \\ \vdots \\ \xi_n(t) \end{matrix}\right\}$$

Substituting equation 8 into 1a and noting conditions 6, the result is a set of uncoupled equations in coordinates ξ (the normal coordinates).

$$\left\{\ddot{\xi}\right\} + \left\{\omega^2 \xi\right\} = 0 \qquad (9)$$

where

$$\left\{\omega^2 \xi\right\} = \left\{\begin{matrix} \omega_1^{\ 2} & \xi_1 \\ \omega_2^{\ 2} & \xi_2 \\ \vdots & \\ \omega_n^{\ 2} & \xi_n \end{matrix}\right\}$$

These are the equations for a set of n uncoupled single degree of freedom undamped oscillators with natural periods (ω_n).

The response in the real system coordinates is obtained from responses of the single degree of freedom systems by a linear combination given by equation 8.

$$\{x\} = [Q]\{\xi\}$$

For the nonhomogeneous case equation 9 becomes

$$\{\ddot{\xi}\} + \{\omega \xi\} = \frac{[Q]^T \{f(t)\}}{[Q]^T [M] [Q]} \tag{10}$$

where

$$\frac{[Q]^T \{f(t)\}}{[Q]^T [M] [Q]} = \{g\} = \text{generalized force.} \tag{10a}$$

For the base acceleration, $\ddot{y}(t)$ assumed in equation 1

$$\{f(t)\} = [M]\ \{-\ddot{y}\}$$

The response in the real system is again given by equation 8 where the $\{\xi\}$ are now obtained from equation 10.

Thus the method consists of breaking the n degree of freedom system given by equation 1 into n single degree of freedom uncoupled systems with natural frequencies given by 4 and forcing functions given by 10a. The desired answer in the real system is then obtained by the relationship 8 where the elements of $\left[Q\right]$ are obtained from 5.

Turning now to a three degree of freedom system and defining

$$\begin{aligned} k_1 &= k & m_1 &= m \\ k_2 &= ak & m_2 &= \alpha m \\ k_3 &= bk & m_3 &= \beta m \end{aligned} \tag{11}$$

the solution of equation 4 will be of the form

$$\omega_i^2 = K_i \frac{k}{m}$$

where K_i is a number, the root of a cubic equation depending only on a, b, α, and β.

Since the mode shape is only defined to within a constant it may be written as

$$\left\{\phi^i\right\} = \left\{ \begin{matrix} 1 \\ 1-K_i \\ \dfrac{a}{\beta}\left(\dfrac{1-K_i}{\dfrac{a+b}{\beta} - K_i}\right) \end{matrix} \right\} \tag{12}$$

The generalized force equation 10a is of the form

$$g_i = G_i\, \ddot{y}(t)$$

where

$$G_i = \frac{aK_i - a - 1 - b\, Q_{3i}}{1 + a(Q_{2i})^2 + b\,(Q_{3i})^2} \tag{13}$$

Q_{ij} being the elements of the $\left[Q\right]$ matrix. This again depends only on the parameters a, b, α, and β.

Given a building type, i.e., relationships between the masses and between the spring constants, the mode shapes and generalized force coefficients (G_i) are uniquely determined. Only the ratio of k/m need be selected to calculate a response of the system to a given input.

If viscous damping is present then a third left hand element appears in equation 1 of the form

$$\left[C\right]\left\{\dot{x}\right\}$$

The general requirement on the damping and therefore on the $\left[C\right]$ matrix for classical normal modes is that the same transformation of coordinates that diagonalizes the $\left[M\right]$ and $\left[K\right]$ matrices must also diagonalize the $\left[C\right]$ matrix;

$$\left[Q\right]^T \left[C\right] \left[Q\right] = \left[\bar{C}\right] \text{ a diagonal matrix} \qquad (14)$$

It has been shown (21) that a linear combination of the damping and mass matrices will produce such a diagonalization. Although this is not the most general result that can be obtained from the statement 14 (22), it is convenient for this discussion.

$$\left[C\right] = \bar{a}\left[M\right] + \bar{b}\left[K\right] \qquad (15)$$

Setting $\bar{b} = 0$ (damping relative to base)

$$\bar{c} \sim \frac{1}{\omega}$$

Setting $\bar{a} = 0$ (damping relative to adjacent mass)

$$\bar{c} \sim \omega$$

Since neither of the above situations occur alone in practice, by using both a and b unequal to zero, a more realistic damping arrangement may be obtained.

Rayleigh (21) states that normal modes are a good approximation, even if condition 14 is not satisfied, as long as the damping is small. This is generally the case in structures; in fact, unless the damping is small the responses would, in general, be reduced to such a point that it would not be of interest to investigate them as far as failure is concerned.

The usual situation would generally be one in which the natural frequency, percent of critical damping, and mode shape would be known for each mode or at least the first few modes. Hence these values could be used directly in the mode solution or mode approximation without being concerned with the original structure. The $\left[Q\right]$ matrix would be obtained from the mode shape. This therefore enables one to find the response in the real structure when only the mode properties are known.

III. EFFECT OF DAMPING

In the model considered viscous damping is assumed; i.e., the damping force is proportional to a constant times a velocity.

The floor responses may be obtained considering only the damping coefficients as defined above; the actual physical damping arrangement need not be known. Other quantities of interest such as shear may then be calculated from this data by making use of the building parameters; for example, the spring constants for the case of shear. However, quantities such as base shear and base moment may also be obtained by considering the inertia forces. The mass distribution would presumably be known and the absolute acceleration of each floor could be obtained from a computer solution or approximately from the spectrum data (discussed in the next section). The base shear could then be obtained by calculating the inertia forces (mass times absolute acceleration) at each floor and summing them down the structure. The base moment would similarly be obtained by multiplying each force by the appropriate moment arm and summing. The way in which the damping forces would enter into these shear moment determinations is not obvious, and will be considered further below.

The inertia force addition method may be desirable if some parameters of the structure are known more accurately than others. For instance, it would be more accurate to calculate base shears by this method if the masses of the building were known more accurately than the interfloor shearing spring constants.

For the undamped case (fig. 1) the base shear is defined as

$$V_B = x_n k_n \tag{16}$$

Summing inertia forces would give the same result.

In figure 2 relative interfloor damping is shown and in figure 3, relative-to-base damping. Summing inertia forces for figure 2 gives

$$\sum_{i=1}^{n} \ddot{\bar{x}}_i m_i = -(x_n k_n + \dot{x}_n c_n) \tag{17}$$

and for figure 3

$$\sum_{i=1}^{n} \ddot{\bar{x}}_i m_i = -(x_n k_n + \sum_{i=1}^{n} \dot{x}_i c_i) \tag{18}$$

If the base shear is defined as the sum of all of the lateral forces on the foundation, then equations 17 and 18 correctly give the base shear for the two cases. Note that the definitions of base shear in the damped cases include the extra terms due to damping, given in the right hand members of equations 17 and 18. The damping in reality does occur within the walls and columns and therefore would be expected to contribute to the shearing force on the foundation.

Neglecting the moment caused by the gravity forces of the floors due to the displacements x_i the base moment in both cases is given correctly by

$$M_B = \sum_{i=1}^{n} \ddot{\bar{x}}_i m_i h_i \tag{19}$$

It may thus be concluded that for any structure of the type assumed (fig. 1) with only damping internal to the structure, the base moment is given by equation 19 and the base shear by

$$V_B = \sum_{i=1}^{n} \ddot{\bar{x}}_i m_i \tag{20}$$

Absolute damping is shown in figure 4, between each floor and a reference point fixed in inertial space. The base shear for this type of damping is the same as in the undamped case (equation 16). Summing the inertia forces, one obtains:

$$\sum_{i=1}^{n} \ddot{\bar{x}}_i m_i = -\left(x_n k_n + \sum_{i=1}^{n} \dot{\bar{x}}_i c_i \right) \tag{21}$$

Therefore the inertia terms in this case will differ from the true shear by

$$\sum_{i=1}^{n} \dot{\bar{x}}_i c_i = \sum_{i=1}^{n} \dot{x}_i c_i + \dot{y} \sum_{i=1}^{n} c_i \tag{22}$$

The base moment for this case is

$$M_B = \sum_{i=1}^{n} \ddot{\bar{x}}_i m_i h_i + \sum_{i=1}^{n} \dot{\bar{x}}_i c_i h_i \tag{23}$$

Therefore moment estimates based on the inertia terms would be in error by

$$\sum_{i=1}^{n} \dot{\bar{x}}_i c_i h_i = \sum_{i=1}^{n} \dot{x}_i c_i h_i + \dot{y} \sum_{i=1}^{n} c_i h_i \tag{24}$$

Absolute damping for a building could occur only as air damping and the error introduced by using inertia forces, to obtain base shear or base moment, would become important only if air damping is an important effect.

The three effects that the air around a building has during vibration are:

1. Increased effective mass
2. Energy radiation
3. Viscous effects

Only the last two cause dissipation of energy and therefore air damping. The first causes only a change in the natural frequency of the system. All the effects can generally be considered negligible for structures and therefore equations 22 and 24 would not apply. To demonstrate this a hypothetical one degree of freedom system was used to compute some typical numerical values as shown in appendix I.

IV. METHODS OF MODE COMBINATION

When a modal analysis of a multidegree of freedom system is used, the n responses of the single degree of freedom modes must be combined using the appropriate participation factors to obtain the desired response in the real system. In general these n functions of time cannot be described by any simple mathematical expression and hence an analytical combination cannot be made. By analog computer methods, however, the correct combination of modes can be obtained.

The information on the individual modes most readily available is generally in the form of response spectra (velocity spectra in most cases). Spectra have been prepared for most strong motion earthquakes (23).

The velocity spectrum of a forcing function (earthquake) is the maximum relative velocity that occurs in a single degree of freedom oscillator (fig. 5) as a function of the natural period of the system for a given damping.

The general response of such a system is

$$\xi_s = \frac{T}{2\pi\sqrt{1-\rho^2}} \int_0^t \ddot{y}(\tau)\, e^{\frac{-2\pi\rho}{T}(t-\tau)} \sin\frac{2\pi}{T}\sqrt{1-\rho^2}\,(t-\tau)\,d\tau \qquad (25)$$

where

$$T = \text{natural period} = 2\pi\sqrt{m/k}$$

$$\rho = \text{damping ratio} = \frac{\text{damping in system}}{\text{critical damping of system}} = \frac{c}{2\sqrt{km}}$$

Assuming small damping ($\sqrt{1-n^2} \approx 1$) and earthquakelike excitation, and differentiating, one obtains

$$\dot{\xi}_s \approx \int_0^t \ddot{y}(\tau)\, e^{-\frac{2\pi\rho}{T}(t-\tau)} \sin \frac{2\pi}{T}(t-\tau)\, d\tau \qquad (26)$$

The velocity spectrum ($S_v(T)$) is defined as $\left|\dot{\xi}_s\right|_{max}$. On this basis the following approximate relationships may be derived (24):

$$\begin{aligned} \left|\xi_s\right|_{max} &= \frac{T}{2\pi} S_v \\ \left|\dot{\xi}_s\right|_{max} &= S_v \\ \left|\overline{\ddot{\xi}}_s\right|_{max} &= \frac{2\pi}{T} S_v \end{aligned} \qquad (27)$$

where $\overline{\ddot{\xi}}_s$ is the absolute acceleration ($\overline{\ddot{\xi}}_s = \ddot{\xi}_s + \ddot{y}(t)$).

It is well to point out that $\left|\overline{\ddot{\xi}}_s\right|_{max}$ is the absolute acceleration spectrum for a single degree of freedom system only. The problem of the use of absolute acceleration spectra for multidegree of freedom systems may be clarified by returning for a moment to the time responses and applying equation 8 to accelerations using relative coordinates:

$$\{\ddot{x}\} = [Q]\{\ddot{\xi}\}$$

but

$$\{\overline{\ddot{x}}\} = [Q]\{\ddot{\xi}\} + \{\ddot{y}(t)\} \qquad (28)$$

The ξ_i are the mode responses to the generalized force g_i (equation 10a). Therefore

$$\xi_i = G_i \; \xi_{si} \tag{29}$$

and

$$\{\ddot{x}\} = [Q] \{G \ddot{\xi}_s\} + \{\ddot{y}(t)\} \tag{30}$$

where

$$\{G \ddot{\xi}_s\} = \begin{Bmatrix} G_1 & \ddot{\xi}_{s1} \\ G_2 & \ddot{\xi}_{s2} \\ \vdots & \\ G_n & \ddot{\xi}_{sn} \end{Bmatrix}$$

Equation 30 indicates that in multidegree of freedom systems the n mode contributions obtained from the relative acceleration spectrum must be combined with the maximum value of the input acceleration to produce the absolute acceleration at some point in the structure.

The absolute acceleration spectra for a single degree of freedom system given by equation 27 may be used as an approximation for the calculation of a multidegree of freedom system. Returning again to the time response

$$\{\ddot{x}\} \approx [Q] \{G \ddot{\bar{\xi}}_s\} = [Q] \{G \ddot{\xi}_s\} + [Q] \{G \ddot{y}(t)\} \tag{31}$$

and comparing equation 30 and 31 it will be seen that equation 31 involves the following error:

$$\left(\sum_{j=1}^{n} Q_{ij} \, G_j - 1 \right) \ddot{y}(t)$$

Thus one can say that $\left| \ddot{x}_i(t) \right|_{max}$ can be obtained for the multidegree of freedom system from the single degree of freedom absolute spectrum of equation 27 provided that $\sum_{j=1}^{n} Q_{ij} \, G_j \approx 1$ or $\ddot{y}(t)$ is small.

Generally the velocity spectrum and hence the displacement and absolute acceleration spectra would be the starting point for the calculation. The n maximum values corresponding to the n modes would thus be known, but all phase and time relationships would be unavailable. The question of how these values should be combined to provide the best estimate of the maximum response then becomes one of critical importance.

The sum of the absolute values of the individual maximum mode responses is the upper limit of the system response.

$$\text{Response} = R = \sum_{i=1}^{n} A_i \, \xi_i(t)$$

$$\left| R \right|_{max} = \left| \sum_{i}^{n} A_i \, \xi_i(t) \right|_{max} \leq \sum_{i}^{n} A_i \left| \xi_i(t) \right|_{max} \qquad (32)$$

The A_i's are coefficients depending on the parameters of the desired structural response. $\dot{\xi}_i(t)$ or $\ddot{\xi}(t)$ may be substituted for $\xi(t)$ giving velocities, approximate accelerations, etc., throughout the structure.

The algebraic sum of the maximum values has also been shown to give good results when the input function is a pulse with the following relationship to structure parameters (16):

$$\frac{2\,t_m}{T_1} > 1 \qquad (33)$$

where T_1 is the fundamental period (sec) and t_m is the rise time of the pulse (sec).

For a typical building T_1 would be one to two seconds, therefore, for the algebraic sum to apply, $t_m > \frac{1}{2}$ second. By inspecting typical earthquake accelerograms it is obvious that earthquakes do not satisfy this condition and hence this method of combination would not be applicable.

A so called "statistical" combination of the spectrum values has been suggested (17). It is obtained by taking the square root of the sum of the squares of the quantities to be combined. If the complete time responses of the modes could be considered as independent functions having Gaussian probability distributions, some conclusions based on a statistical analysis could be made. The distributions of $\xi_i(t)$ would be of the form:

$$\phi(\xi) = \frac{1}{\sigma\sqrt{2\pi}} \; e^{-(x-a)^2/2\sigma^2} \tag{34}$$

where a is the mean (zero in this case) and σ^2 is the variance. The expected value is

$$E(\xi) = \int_{-\infty}^{\infty} \frac{x\,e^{-x^2/2\sigma^2}}{\sigma\,\sqrt{2\pi}}\,dx \tag{35}$$

$$E\,|\xi| = 2E(t\,\xi) = \sigma\sqrt{2/\pi} \tag{36}$$

For independent Gaussian functions it is well known that (24)

$$\sigma_T{}^2 = \sigma_1{}^2 + \sigma_2^2 + \ldots\ldots + \sigma_n{}^2 \tag{37}$$

where $\sigma_T{}^2$ is the variance of the total response made up of the n mode responses each with variance σ_i^2.

Applying 37 to 36

$$E\left|x\right|_{total} = \sqrt{\sum_{i=1}^{n} (E\left|\xi_i\right|)^2} \tag{38}$$

Also

$$\sigma^2 = E(x)^2 - (E(x))^2 \tag{39}$$

where $E(x)^2$ is the mean square. Applying equation 37

$$RMS_{total} = \sqrt{\sum_{i=1}^{n} (RMS)_i^2} \tag{40}$$

The above applies only if the input functions are Gaussian since the output of a linear system in this case is also Gaussian. The extent to which typical earthquakes will satisfy these conditions is not as yet completely known. On the basis of an investigation of a group of typical earthquake accelerograms (refer to appendix II) the assumption of a Gaussian model would seem a reasonable one. In the earthquake situation the responses $\xi_i(t)$ are generated from the same input function, which would indicate that the functions are not independent. However, for systems with well spaced natural frequencies and an input function with a peaked power spectrum, it can be shown under some conditions that the mode responses may be considered independent (26).

The actual quantities occurring in practical structural calculations are not the root mean square values (RMS) or the expected absolute values, but the maxima of the functions $\xi_i(t)$. However, equations 38 and 40 may be considered as indications that the application of the relation

$$R_{(\text{maximum structure})} = \sqrt{\sum_{i=1}^{n} (R_{i\,(\text{maximum mode})})^2} \tag{41}$$

might provide a useful form for an "empirical" relationship and its validity checked experimentally. This is the point of view adopted here.

It is of interest to consider the possible error involved in using the above methods of combination. The absolute value of the true response could conceivably lie anywhere from zero to the value obtained by adding the absolute values of each mode. The sum of the absolute values thus could never err on the nonconservative side but could approach infinite percentage error on the conservative side.

The square root of the sum of the squares can also approach infinite percentage error on the conservative side but it may also err on the nonconservative side. The maximum nonconservative error would occur when the true value is equal to the sum of the absolute values.

$$R_t = a + b + c \tag{42}$$

where R_t is the true response and a, b, c are the mode responses for a three degree of freedom system. This may be seen by noting that for a given set of values (a, b, c) the square root of the sum of the squares will be the same regardless of the true value (R_t). The true value, however, may range from zero to the absolute sum and hence the largest non-conservative error occurs when R_t is at the upper bound as given in equation 42.

Let a be the largest value and

$$\begin{aligned} b &= \alpha a \\ c &= \beta a \end{aligned} \tag{43}$$

therefore

$$\alpha \text{ and } \beta \leq 1$$

and

$$R_t = (1 + \alpha + \beta)a$$

The square root of the sum of the squares (R_{srs}) is

$$R_{srs} = \sqrt{a^2 + b^2 + c^2} = \sqrt{a^2(1 + \alpha^2 + \beta^2)} \tag{44}$$

The nonconservative error ($E_n(\%)$) is then given by:

$$E_n = \left(\frac{R_t - R_{srs}}{R_t} \right) 100 \tag{45}$$

Substituting

$$E_n = \left(1 - \sqrt{\frac{1+\alpha^2+\beta^2}{(1+\alpha+\beta)^2}} \right) 100 = \left(1 - \sqrt{\frac{(1+\alpha^2+\beta^2)}{(1+\alpha^2+\beta^2) + (2\alpha+2\beta+2\alpha\beta)}} \right) 100$$

Since α and $\beta \leq 1$ the maximum nonconservative error occurs when all modes have equal contributions ($\alpha=\beta=1$):

$$E_{n\ max} = \left(1 - \frac{1}{\sqrt{3}} \right) 100$$

Generalizing to n modes in combination:

$$E_{n\ max} = \left(1 - \frac{1}{\sqrt{n}} \right) 100 \tag{46}$$

An average or a weighted average (R_{avg}) of the sum of absolute values and the square root of the sum of the squares might also be a useful form:

$$R_{avg} = \frac{\sqrt{a^2+b^2+c^2} + m(a+b+c)}{m+1} \tag{47}$$

where m is a weighting factor.

$$E_{n\ max} = \left(\frac{R_t - R_{avg}}{R_t}\right)100 = \left(1 - \left[\frac{1}{m+1\sqrt{n}} + \frac{m}{m+1}\right]\right)100 \qquad (48)$$

The maximum again occurs when all the modes have equal contributions. Equation 48 reduces to 46 at $m = 0$ and a straight average occurs at $m = 1$.

Equation 48 shows that by properly choosing m one can limit the amount of possible nonconservative error to any desired value at the expense of increasing the conservative error. It also shows that the larger the number of degrees of freedom of the system considered, the larger the possible nonconservative error, and the closer one must approach the sum of absolute values to insure a specified nonconservative error.

In the above analysis certain extreme cases have been considered, which may not always be good approximations to actual situations. As will be seen in later sections, the upper bound may be closely approached. The true response R_t may be of the order of ninety five percent of the sum of the absolute values. The assumption of equal mode contributions will be shown in some cases to be a poor approximation. A more realistic relation of the three mode contributions in the case of base shear for a three degree of freedom system would be in the ratio 5:3:1, the first mode being the largest contributor. Evaluating equation 48 using the above modifications, i.e.,

$$R_t = 0.95(a + b + c)$$

$$\alpha = 3/5$$

$$\beta = 1/5$$

would give

$$E_{n\,max} = \left(1 - \frac{1}{0.95}\left[\frac{0.658}{m+1} + \frac{m}{m+1}\right]\right) 100 \tag{49}$$

The weighting factor m would be chosen to keep the maximum possible nonconservative error in the desired range. Equation 49 indicates that for a direct average (m=1) the negative error would be less than 12.8 percent and for the square root of the sum of the squares (m=0) the negative error would be less than 30.7 percent. Using the first mode alone, as an approximation to the total response, the maximum negative error would be less than 41.5 percent, under the above assumptions. The average of the first mode and the sum of the absolute values, which is identical to taking the full value of the first mode plus one half of the contribution of each higher mode, would have a maximum negative error less than 18.1 percent. These above ranges are consistent with experimental results given later in this thesis.

V. EXPERIMENTAL SETUP

Versatility, reasonable operating speed and accuracy commensurate with an engineering type problem were the main factors governing the selection of the computing system. A mechanical analog would tend to be cumbersome and slow and accuracy could be impaired by mechanical details for multidegree of freedom systems. A digital solution has versatility depending on the magnitude of the program and in turn on the capacity of the machine. The processing of the input data becomes troublesome and the accuracy of a digital machine is of no particular advantage since the input and the parameters of a real structure are in general not exactly known. A passive analog would require auxiliary amplifiers to produce the zero damping state and is laborious to set for different conditions unless specially coupled inductances and resistances are used (4). This increased speed and complication is not warranted since a complete spectrum entailing a large number of points is not required.

All of the above methods would, of course, give the desired results, but for the above reasons and the circumstance of availability of active elements, a special purpose electronic differential analyzer was assembled. Three degrees of freedom were used although the system need not have been limited to this number. The computer can thus be considered as either a complete three degree of freedom system or as a three degree of freedom approximation to a larger system.

A photograph of the setup, (fig. III-1), as well as an overall diagram and diagrams of individual components are given in appendix III.

The equation to be solved in each mode of the analog is

$$\ddot{\xi}_i = -2\rho\omega_i\dot{\xi}_i - \omega_i^2\xi_i + G_i\ddot{y}(t) \tag{50}$$

This may also be written in terms of the previously defined nomenclature as

$$\ddot{\xi}_{si} = -2\rho\omega_i\dot{\xi}_{si} - \omega_i^2\xi_{si} + \ddot{y}(t) \tag{51}$$

ξ_i is the ith mode response and ξ_{si} the response of the corresponding single degree of freedom system to $\ddot{y}(t)$. (It is the maximum value of ξ_{si} that is obtained from the response spectrum curve.) By using form 51 all the modes can be excited with the same input and no input coefficient potentiometers are required (fig. III-2). The response in the real system is

$$x_i = \sum_j Q_{ij}\, G_j\, \xi_{sj} \tag{52}$$

Details of the operation of the computer and a discussion of experimental accuracy are given in appendix III.

If absolute damping is desired, the equation to be solved takes the form:

$$\ddot{\xi}_i = -2\rho_i\omega_i\dot{\xi}_i - \omega_i^2\xi_i + G_i(\ddot{y}(t) + \epsilon\dot{y}) \tag{53}$$

where

$$\epsilon = 2\rho_i\omega_i Q^{-1}$$

If the system is such that classical normal modes cannot be obtained, then the computer method may still be used. A simplification in the computer may be obtained by first making the same transformation as given in the general equation section. The spring and mass matrices will then be diagonal and there will only be cross coupling in the velocity (damping) section of each mode because the damping matrix is no longer diagonal.

VI. EXPERIMENTS CONDUCTED

To examine various mode combination possibilities three earthquakes were chosen as typical inputs:

1. Short time duration (approximately five seconds)
   San Francisco (Golden Gate Park) N10E, March 22, 1957, (N = 307)
2. Medium time duration (approximately nineteen seconds)
   Taft N21E, July 21, 1952, (N = 341)
3. Long time duration (approximately twenty-seven seconds)
   El Centro EW May 18, 1940, (N = 416)

The ground accelerograms for these earthquakes are shown in figure IV-1.

Three building types were chosen to give representative examples for checking the various methods of combination. In the notation of equation 11 they are:

1. Uniform

$$a = b = \alpha = \beta = 1$$

2. Uniform taper

$$a = \alpha = 2 \qquad b = \beta = 3$$

3. Step

$$a = b = \alpha = \beta = 2$$

The $\left[Q\right]$ matrices, G_i, etc., for each case are given in appendix IV.

Three cases of damping were chosen.

1. All modes 0%
2. First mode 2.5%, second and third 5%
3. All modes 5%

The Alexander building in San Francisco is the only structure for which complete dynamic properties and a measured response to an earthquake are available. The Alexander building is a fifteen story structure 60 feet by 68 feet by 197 feet high with a fundamental period of 1.27 seconds (27). The computer was used to obtain a three degree of freedom approximation to this larger system and various responses in the structure were checked.

A set of results for four, eight, and sixteen story shear structures has been obtained by Jennings (7) using a digital computer. The damped cases chosen in these studies were of the absolute type and the parameters chosen resulted in systems not having classical normal modes. In some cases there is uncertainty as to the acceleration inputs used in this work. It was possible, however, to check the zero damped case for one earthquake to compare the results directly with those of this thesis. In this comparison three degrees of freedom were used to approximate an eight story structure.

The mode shapes, frequencies, etc., required to set up a three degree of freedom approximation for the Alexander building and the comparison case of Jennings, are given in appendix IV.

VII. RESULTS

A complete set of data for the nine cases of building types, earthquakes, and dampings was obtained. Not all of the data was required for the purposes of this thesis but is included for future reference. The unreduced data is presented with the method of reduction at the end of appendix IV. Oscilloscope photographs of sample responses for the three modes of displacements (fig. IV-2), velocities (fig. IV-3), and accelerations (fig. IV-4), are given in appendix IV, along with a trace of typical complete responses (fig. IV-5).

Five values of the fundamental frequency were chosen for each case, the second and third mode frequencies being related to the fundamental according to the building type.

Figures 6 through 10 show the base shear obtained from the computer, the absolute sum of the mode contributions, and the square root of the sum of the squares of the mode contributions. Table 1 gives the percentage deviation from the computer solution of the latter two methods of mode combination and of the average of these two methods along with the percentage deviation for the first mode alone and the average of the first mode and the sum of the absolute values. It also includes the numerical values of the computer solution and histograms of the deviations for the various methods of combination.

It is seen that the sum of the absolute values may be very conservative and the square root of the sum of the squares very nonconservative. The average of these can be seen to give very good results as far as eliminating errors on the nonconservative side, as indicated by equation 49. The base shears have been considered because of their special interest for the structural design problem, but any other type of response could be similarly represented using the data in appendix IV.

Table 2 shows the base moments obtained from a complete computer solution and those obtained from the first mode contribution only. The fact that the first mode alone is a good approximation was suggested by the form of the coefficients of the base moment equation (III-12) when evaluated for the three types of structures assuming an equal distance (h) between floors.

$$M_B \approx \text{Constant}\ (\ddot{\xi}_{a1} + \ddot{y}) \tag{54}$$

The general applicability of equation 54 would seem likely since the higher modes have both a positive and negative contribution with the possibility of a small net moment in comparison to the first mode's contribution. The three cases cover the types of three story structures generally encountered and results show equation 54 to be a very good approximation. For a particular case equation III-12 would be evaluated to determine the constants and the applicability of 54 could therefore be determined by inspection. This approximation is a useful one in that it requires only a knowledge of the absolute acceleration spectrum and hence the velocity spectrum for a single degree of freedom system (refer to equation 25).

Figure 11 shows the velocity spectrum points obtained directly from the computer compared to the same points obtained from the displacement and acceleration spectrum points. This is, therefore, a check on equation 27. The results support the validity of these relationships for earthquakelike functions.

Table 3 gives the results of the check of the Alexander Building. The computer values (three degree approximations) are seen to check very well with the measured values and the mode contributions check well with those computed using the spectrum data from a passive analog (28). The combinations using these mode results are subject to the approximations given in equation 31. The direct average of the absolute sum and square root of the sum of the squares again gives a safe and usable result. Three modes in this case were ample to give a good approximation. For most earthquakes the spectrum curves are defined within the range of periods from 0.1 to 3 seconds and for typical structures this range will ordinarily not include more than three modes. In general velocity spectra curves decrease rapidly below a period of the order of 0.3 seconds.

The one example of an eight story building chosen from Jennings' work resulted in a base shear value from the three mode approximation of 2780 Kips. Jennings' value, computed using a digital machine, was 2537.54 Kips. This is a good agreement considering the many possible differences in input data and types of approximation.

VIII. CONCLUSIONS

The results of the study of various methods of mode combination for the assumed structural models and earthquake excitations are:

1. The sum of the absolute values ranged from 0.7% to 84% greater than the computer solution. A significant feature is the distribution of values which is shown in the histogram of table 1. This indicates that ninety percent of the values were in the range from 0.7% to 50% greater and fifty percent of the values were in the range from 0.7% to 20% greater than the computer solution. The steep front on the histogram indicates that a relatively large number of the absolute sums are fairly close to the true value.

2. The square root of the sum of the squares ranged from 24% less to 32% greater than the computer solution. The predicted maximum negative deviation is 30.7%. Refer to the histograms of table 1 for details on this and the following cases.

3. The average of the sum of the absolute values and the square root of the sum of the squares ranged from 11% less to 58% greater than the computer solution. The predicted maximum negative deviation is 12.8%.

4. The values of the first mode ranged from 37% less to 28% greater than the computer solution. The predicted maximum negative deviation is 41.5%.

5. The average of the first mode and the sum of the absolute values

ranged from 13% less to 54% greater than the computer solution. The predicted maximum negative deviation is 18.1%. All of the methods have a similar spread of values; the maximum nonconservative error is the distinguishing feature. In general, any reduction in the conservative error of the sum of the absolute values is made at the expense of increasing the probable magnitude of nonconservative error.

A weighted average of methods one and two above permits a choice of the allowable nonconservative error between the extremes. The weighted average method may be preferable in some design situations to any simple summation since the values on the average are closer to the true response and yet are within the limit of maximum nonconservative error prescribed by the weighting function. The direct average is a special case of this with the weighting function taken as unity. For critical designs, where no negative error can be tolerated, this average reduces to the sum of the absolute values.

The response of the first mode gives a good approximation to the base moment. This requires only the use of the absolute acceleration spectrum for a single degree of freedom system.

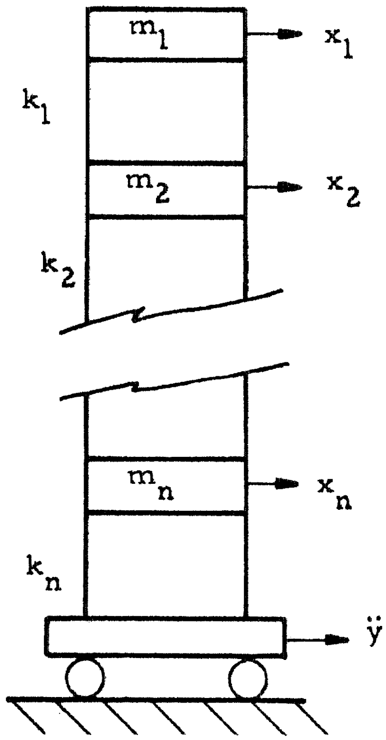

x_i relative coordinates

m_i concentrated masses

k_i spring constants in shear between floors i and i + 1

$\ddot{y}$ base acceleration

Figure 1

Shear Building Model

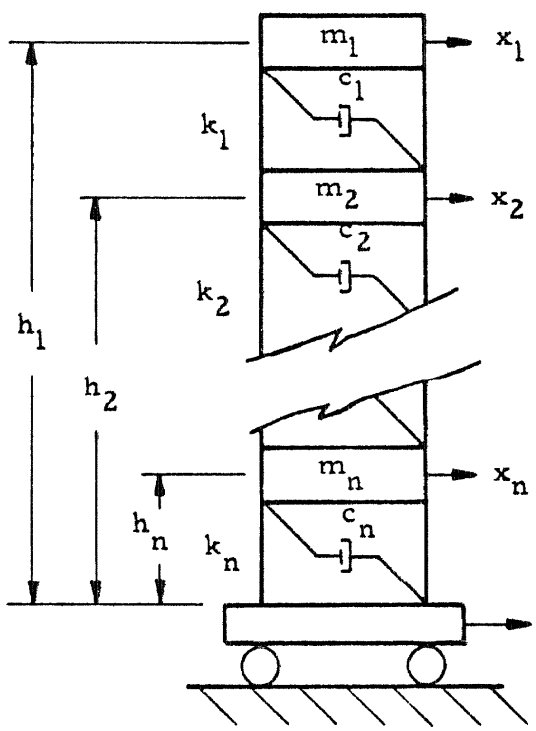

Figure 2

Relative Interfloor Damping

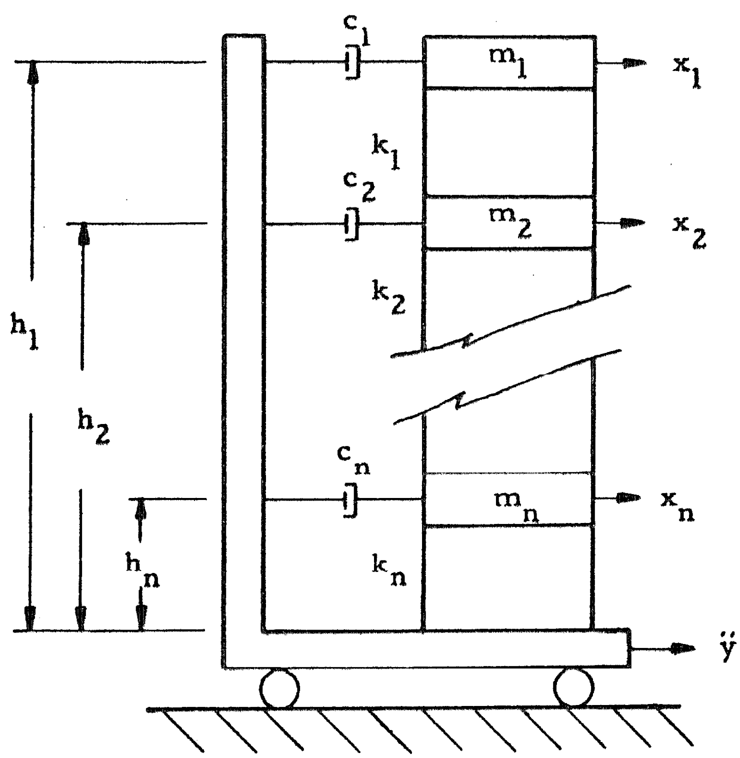

Figure 3

Relative-to-base Damping

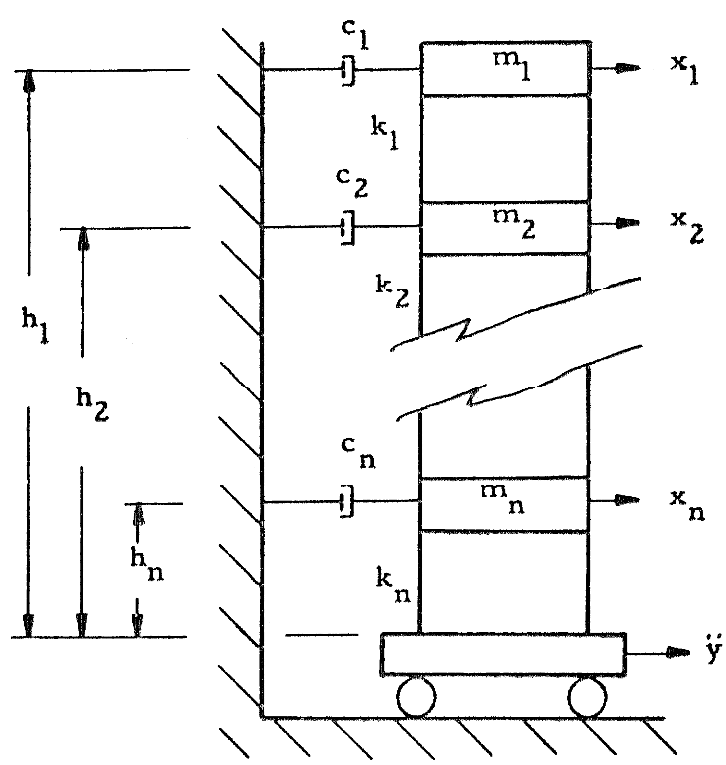

Figure 4

Absolute Damping

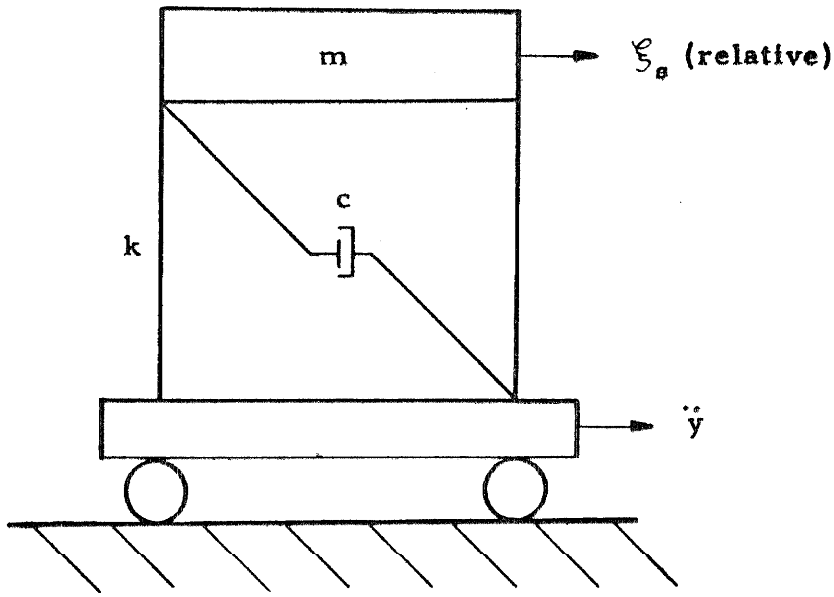

Figure 5

Spectrum Model

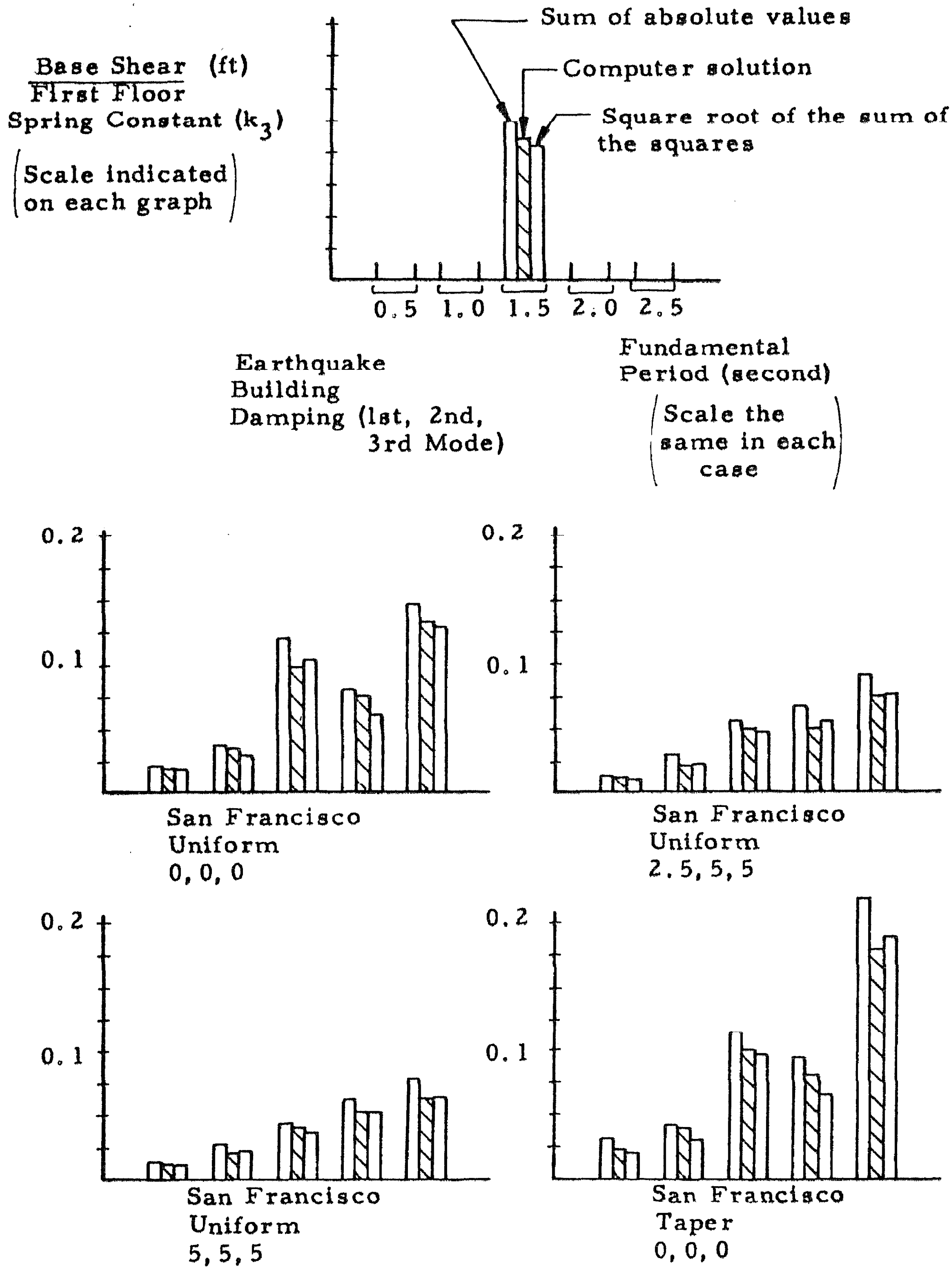

Figure 6

Base Shear

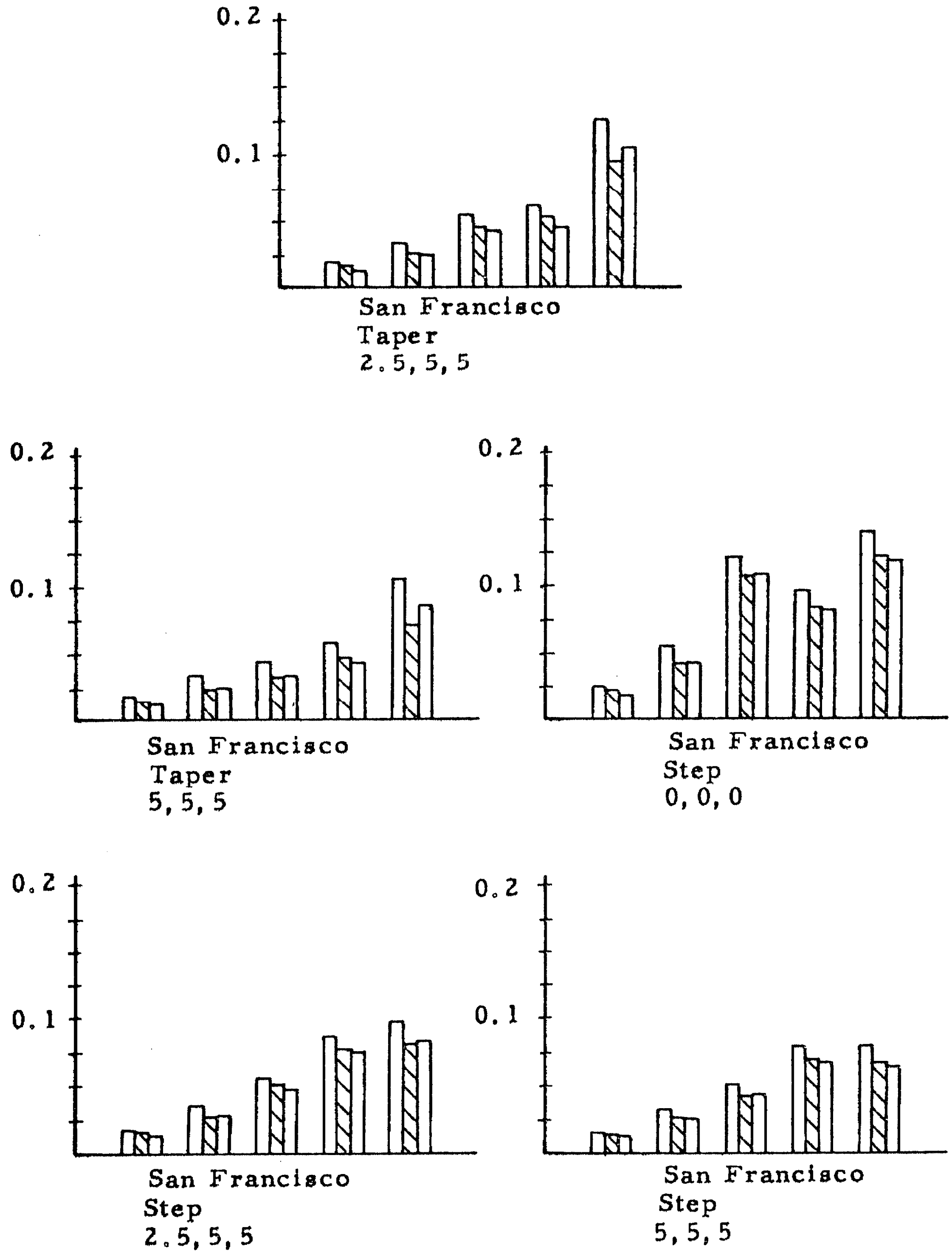

Figure 7

Base Shear

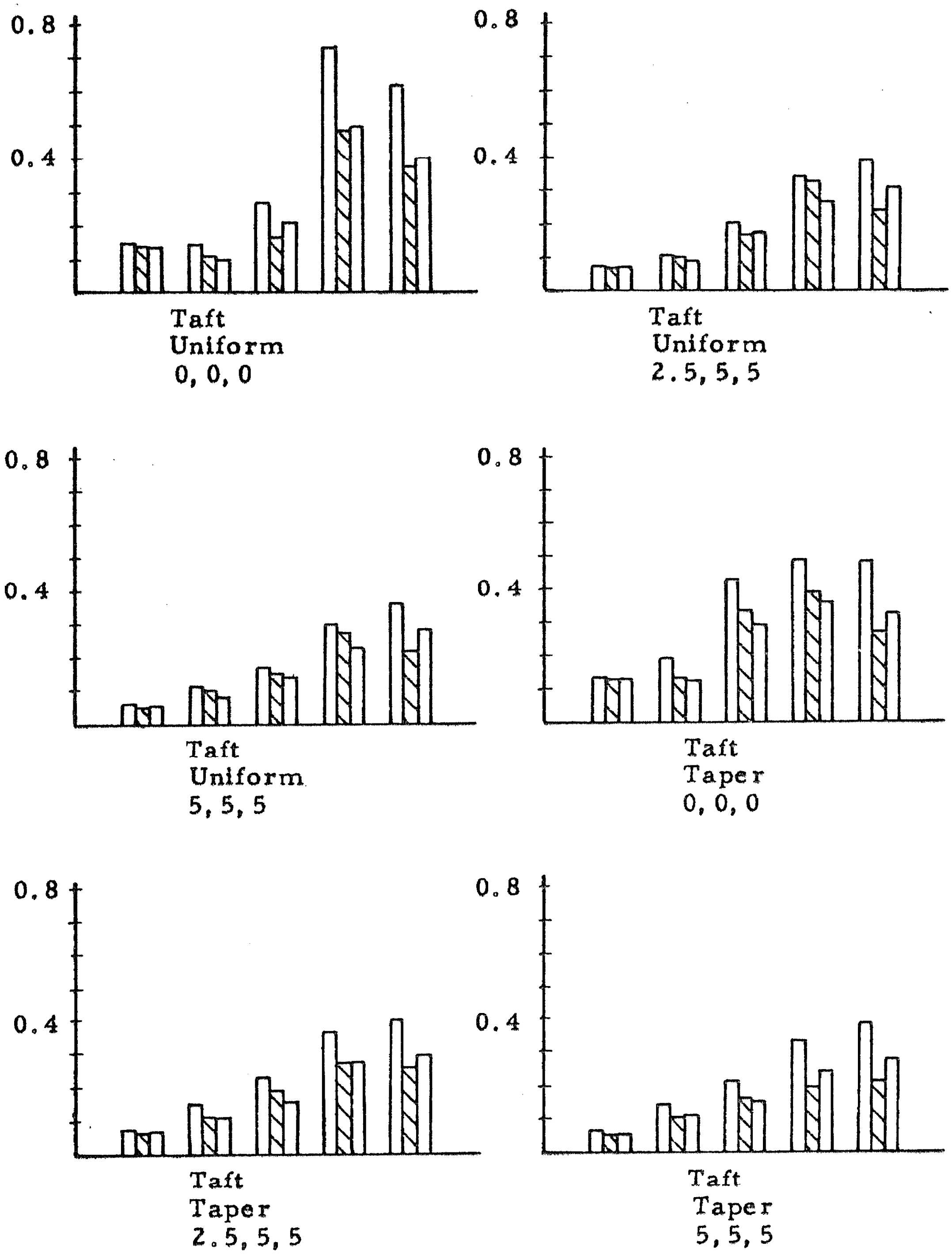

Figure 8

Base Shear

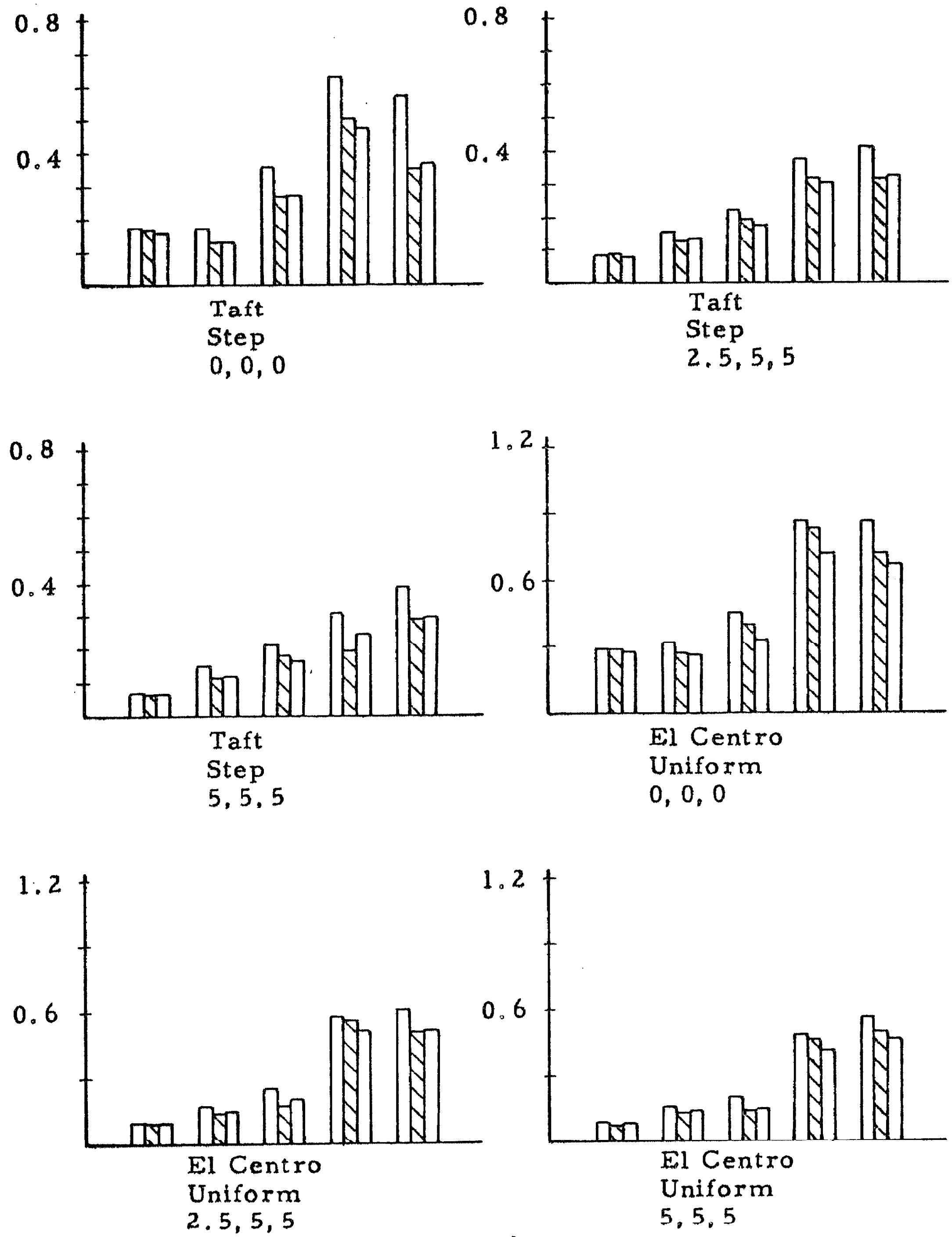

Figure 9

Base Shear

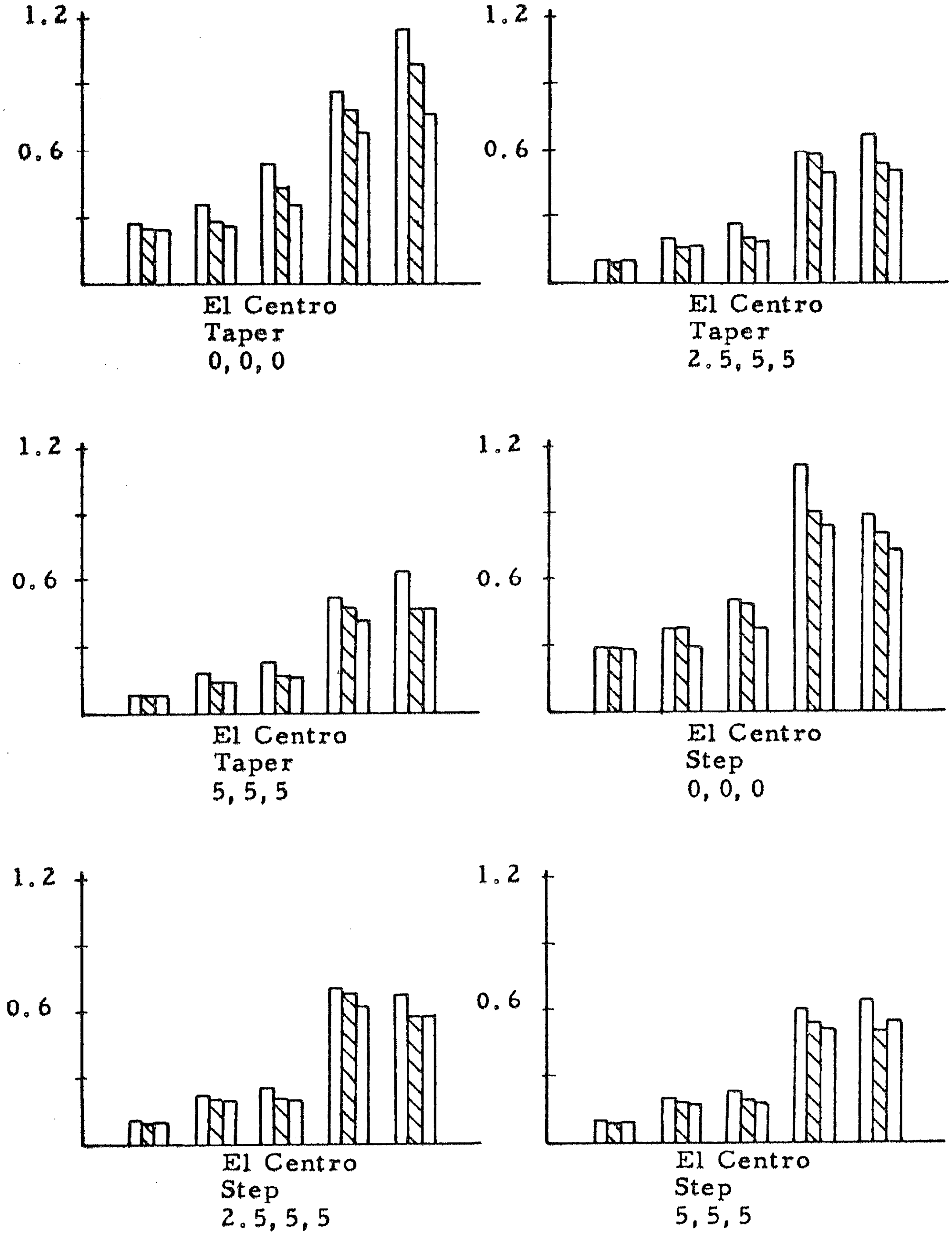

Figure 10

Base Shear

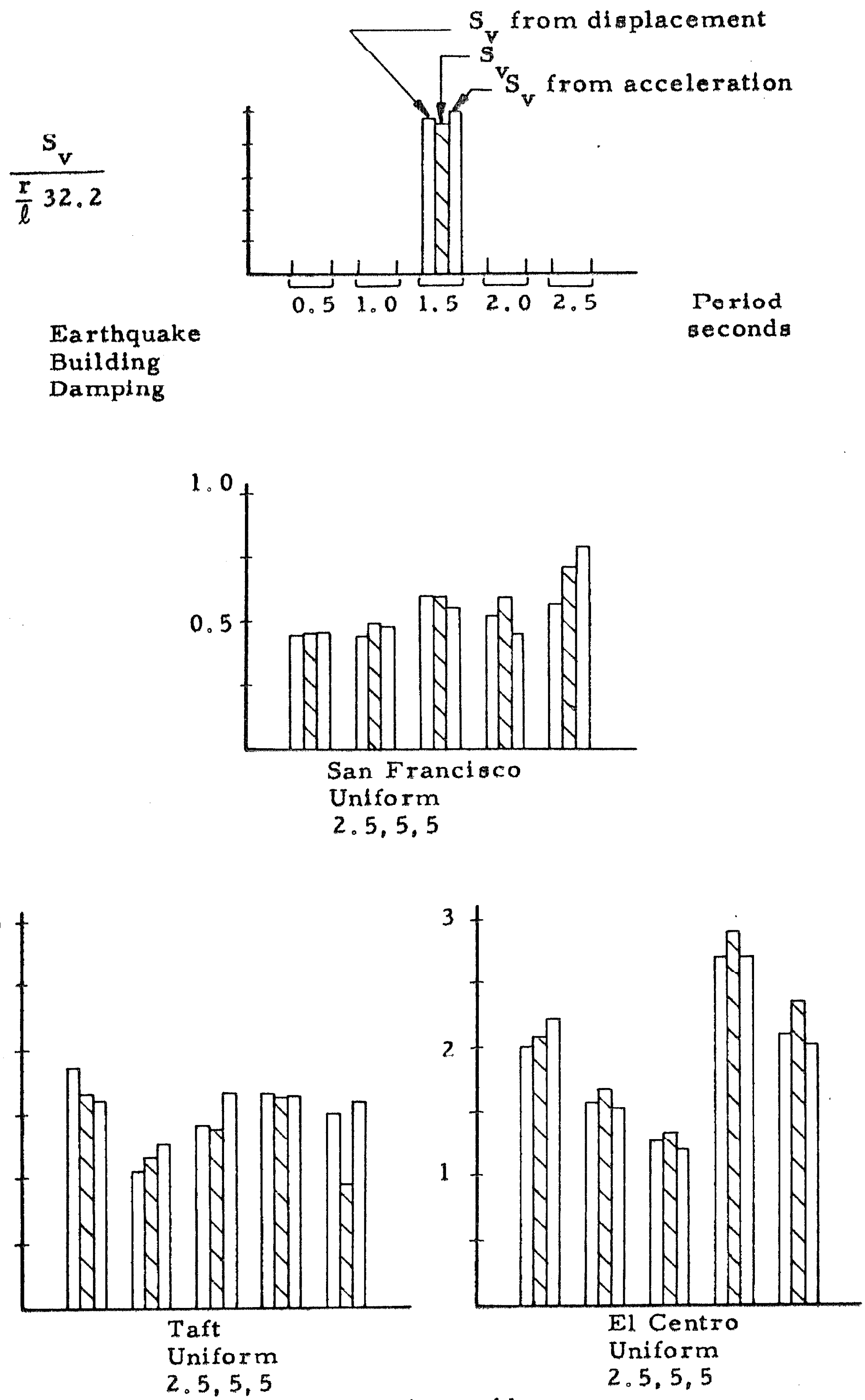

Figure 11

Velocity Spectrum Comparison

TABLE 1

Percentage Comparison of Methods of Combination

Notations used in this table are:

comp	=	computer summed result. Numerical values given are $\dfrac{\text{Base Shear}}{\text{First Floor Spring Constant } (k_3)}$
sum	=	deviation of the sum of the absolute values from the computer solution (%)
avg	=	deviation of the value obtained by taking the direct average of the square root of the sum of the squares and the sum of the absolute values from the computer solution (%)
srs	=	deviation of the square root of the sum of the squares from the computer solution (%)
fm	=	deviation of the value of the first mode from the computer solution (%)
fma	=	deviation of the average of the first mode and the sum of absolute values from the computer value (%)
T	=	fundamental period (sec)
a, b, c%	=	percent of critical damping in the first (a), second (b), and third (c) modes

TABLE 1 (Continued)

San Francisco Earthquake

T	2.5	2.0	1.5	1.0	0.5
Uniform building					
0, 0, 0%					
comp	0.1325	0.0765	0.0970	0.0357	0.0204
sum	11.1	5.6	23.7	9.2	18.6
avg	4.0	-6.9	15.2	-4.8	9.8
srs	-3.7	-19.5	6.6	-18.4	1.2
fm	-3.8	-23.4	5.1	-21.5	0.0
fma	3.8	-8.9	14.4	-6.2	9.3
2.5, 5, 5%					
comp	0.0765	0.0510	0.0510	0.0230	0.0143
sum	21.0	33.0	10.8	36.0	1.6
avg	11.3	22.3	3.3	21.5	-5.8
srs	1.4	11.6	-4.1	7.0	-13.3
fm	0.0	10.0	-4.9	4.3	-14.0
fma	10.6	21.4	3.0	20.0	-6.3
5, 5, 5%					
comp	0.0612	0.0510	0.0408	0.0209	0.0128
sum	26.3	22.9	7.4	31.6	13.6
avg	14.3	12.3	-1.2	18.7	5.0
srs	2.3	1.8	-10.8	5.8	-3.5
fm	0.0	0.0	-12.5	2.4	-4.3
fma	13.2	11.5	-2.4	17.0	4.7
Tapered building					
0, 0, 0%					
comp	0.1795	0.0801	0.1040	0.0401	0.0236
sum	21.3	16.8	11.5	3.7	33.5
avg	13.5	-0.1	1.9	-10.3	12.5
srs	5.6	-17.0	-7.7	-24.2	-8.5
fm	4.5	-23.6	-9.3	-29.6	-26.2
fma	12.7	-3.4	0.9	-13.0	3.6
2.5, 5, 5%					
comp	0.0945	0.0520	0.0449	0.0265	0.0166
sum	33.0	16.7	20.9	27.9	17.4
avg	22.2	1.5	8.6	13.0	0.6
srs	11.3	-13.7	-3.8	-1.9	-15.6
fm	10.1	-18.5	-5.6	-5.7	-23.5
fma	21.5	-0.7	7.6	11.3	-3.0
5, 5, 5%					
comp	0.0710	0.0472	0.0331	0.0236	0.0142
sum	50.3	23.6	38.0	37.7	23.2
avg	36.0	7.2	20.7	21.0	4.9
srs	22.0	-9.3	3.5	4.3	-13.4
fm	19.7	-15.0	-0.3	0.0	-24.0
fma	35.2	4.3	17.7	18.9	-0.4

TABLE 1 (Continued)

T	2.5	2.0	1.5	1.0	0.5
Stepped building					
0, 0, 0%					
comp	0.1240	0.0832	0.1080	0.0431	0.0226
sum	14.5	16.0	12.0	27.9	11.1
avg	5.2	7.0	6.0	14.7	-0.7
srs	-4.0	-2.0	0.0	1.9	-12.4
fm	-4.8	-3.0	-0.5	-0.2	-14.2
fma	4.8	6.5	5.7	13.9	-1.3
2.5, 5, 5%					
comp	0.0809	0.0780	0.0511	0.0274	0.0161
sum	22.5	11.8	10.8	26.6	7.5
avg	13.3	4.5	3.1	15.2	-3.4
srs	4.0	-2.8	-4.5	3.7	-14.3
fm	3.0	-3.6	-5.3	2.2	-16.1
fma	12.8	4.1	2.7	14.6	-4.4
5, 5, 5%					
comp	0.0674	0.0700	0.0420	0.0264	0.0135
sum	19.7	13.2	21.7	23.1	8.2
avg	8.5	5.1	12.5	11.2	-4.4
srs	-2.7	-3.0	3.3	-0.8	-17.1
fm	-4.3	-3.9	2.4	-2.3	-20.0
fma	7.4	4.7	12.1	10.4	-5.9

Taft Earthquake

T	2.5	2.0	1.5	1.0	0.5
Uniform building					
0, 0, 0%					
comp	0.3760	0.4850	0.1650	0.1100	0.1420
sum	54.2	50.0	59.4	30.0	7.8
avg	30.2	26.3	42.4	10.9	2.5
srs	6.7	2.7	25.4	-8.2	-2.8
fm	-17.0	-13.2	22.4	-25.0	-3.1
fma	24.0	18.6	41.0	2.9	2.4
2.5, 5, 5%					
comp	0.2290	0.3210	0.1650	0.1010	0.0732
sum	67.8	5.9	22.2	6.9	5.4
avg	52.0	-5.6	11.9	-4.0	2.7
srs	32.3	-17.1	1.7	-14.8	0.3
fm	28.0	-20.2	0.0	-18.3	0.1
fma	48.0	-7.2	11.1	-5.8	2.6
5, 5, 5%					
comp	0.2200	0.2750	0.1560	0.1010	0.0595
sum	66.4	7.3	11.5	7.9	6.2
avg	48.2	-5.7	1.0	-3.5	3.2
srs	30.0	-18.5	-9.6	-14.9	0.2
fm	25.0	-23.3	-11.9	-18.3	0.0
fma	45.5	-8.0	-0.1	-5.8	3.1

TABLE 1 (Continued)

T	2.5	2.0	1.5	1.0	0.5
Tapered building					
0, 0, 0%					
comp	0.2720	0.3900	0.3300	0.1315	0.1270
sum	78.1	24.8	30.6	42.4	7.9
avg	49.0	8.3	9.3	18.9	3.9
srs	19.7	-7.2	-12.1	-4.5	0.0
fm	5.9	-11.0	-35.8	-16.4	0.0
fma	42.0	6.9	-2.6	13.5	3.9
2.5, 5, 5%					
comp	0.2540	0.2720	0.1870	0.1100	0.0635
sum	57.5	32.7	19.8	34.5	18.0
avg	35.6	16.4	2.1	17.7	12.5
srs	13.8	0.0	-15.5	0.9	7.1
fm	6.4	-3.7	-23.0	-3.6	6.6
fma	32.0	14.7	-1.6	15.5	12.3
5, 5, 5%					
comp	0.2120	0.1950	0.1610	0.1030	0.0551
sum	84.4	67.7	33.5	38.8	12.9
avg	58.1	45.4	13.4	21.3	6.6
srs	32.0	23.1	-6.8	3.9	0.4
fm	23.6	16.9	-15.5	-1.9	-0.2
fma	54.0	42.3	9.3	18.9	6.3
Stepped building					
0, 0, 0%					
comp	0.3540	0.5020	0.2760	0.1280	0.1675
sum	61.0	26.3	30.2	36.7	1.8
avg	32.8	10.6	15.2	19.5	-2.1
srs	4.8	-5.2	0.0	2.3	-6.0
fm	-8.2	-11.8	-3.6	-3.1	-6.0
fma	26.4	7.3	13.4	16.8	-2.1
2.5, 5, 5%					
comp	0.3150	0.3150	0.1970	0.1230	0.0827
sum	29.5	18.1	12.7	24.4	0.7
avg	15.9	6.8	1.0	14.8	-1.9
srs	2.2	-4.5	-10.7	5.3	-4.6
fm	0.0	-6.4	-12.2	4.1	-4.7
fma	14.8	5.9	0.3	14	-2.0
5, 5, 5%					
comp	0.2960	0.1970	0.1820	0.1180	0.0690
sum	31.1	59.0	13.7	22.9	3.6
avg	16.6	41.3	1.4	12.7	0.4
srs	2.0	23.8	-11.0	2.5	-2.8
fm	-0.3	19.8	-13.7	1.7	-2.9
fma	15.4	39.4	0.0	12.3	0.3

TABLE 1 (Continued)

El Centro Earthquake

T	2.5	2.0	1.5	1.0	0.5
Uniform building					
0, 0, 0%					
comp	0.7100	0.8290	0.4060	0.2710	0.2880
sum	21.7	5.1	12.5	17.7	1.7
avg	8.0	-4.7	-2.0	7.9	-1.9
srs	-5.8	-14.5	-16.4	-1.8	-5.6
fm	-9.6	-16.3	-20.9	-3.3	-6.3
fma	6.1	-5.6	-4.2	7.2	-2.2
2.5, 5, 5%					
comp	0.5070	0.5580	0.1690	0.1440	0.1010
sum	20.9	4.3	49.6	20.8	5.0
avg	11.1	-2.2	32.5	14.0	2.5
srs	1.4	-8.6	15.4	6.2	0.0
fm	-0.2	-9.3	10.1	5.5	0.0
fma	10.3	-2.4	29.9	13.5	2.5
5, 5, 5%					
comp	0.4900	0.4560	0.1350	0.1300	0.0810
sum	14.9	5.5	49.5	20.8	10.5
avg	5.0	-2.3	29.6	12.7	7.4
srs	-4.9	-10.1	9.6	4.6	4.3
fm	-6.9	-11.2	0.0	3.7	4.3
fma	3.0	-2.7	24.8	12.2	7.4
Tapered building					
0, 0, 0%					
comp	0.9830	0.7800	0.4360	0.2810	0.2500
sum	16.5	11.2	24.3	28.4	12.8
avg	-3.1	-0.5	2.8	10.8	5.2
srs	-22.7	-12.2	-18.8	-7.1	-2.4
fm	-36.5	-14.1	-28.4	-13.9	-3.2
fma	-10.1	-1.4	-2.0	7.3	4.8
2.5, 5, 5%					
comp	0.5300	0.5760	0.1980	0.1560	0.0936
sum	26.0	3.5	30.8	25.0	13.8
avg	9.8	-5.6	11.9	11.5	8.7
srs	-6.4	-14.8	-7.1	-1.9	3.6
fm	-11.7	-16.0	-13.1	-6.4	3.2
fma	7.2	-6.2	8.8	9.3	8.5
5, 5, 5%					
comp	0.4680	0.4680	0.1685	0.1465	0.0765
sum	35.9	10.7	40.0	25.1	11.0
avg	17.8	-0.3	18.4	10.5	4.8
srs	-0.4	-11.3	-3.3	-4.1	-1.4
fm	-6.84	-13.2	-11.9	-8.2	-2.0
fma	14.5	-1.3	14.3	8.6	4.5

TABLE 1 (Continued)

T	2.5	2.0	1.5	1.0	0.5
Stepped building					
0, 0, 0%					
comp	0.8090	0.8990	0.4850	0.3770	0.2870
sum	9.7	24.4	3.9	0.8	0.7
avg	-0.1	8.6	-9.3	-11.3	-1.2
srs	-9.8	-7.1	-22.5	-23.3	-3.1
fm	-11.3	-10.4	-26.0	-26.3	-3.1
fma	-0.8	7.0	-11.1	-12.9	-1.2
2.5, 5, 5%					
comp	0.5750	0.6820	0.2060	0.1975	0.1060
sum	18.8	3.2	24.3	10.1	6.6
avg	9.8	-3.4	11.5	3.0	4.2
srs	0.9	-10.0	-1.9	-4.0	1.9
fm	0.2	-10.6	-4.4	-4.6	1.9
fma	9.3	-3.7	9.9	2.8	4.2
5, 5, 5%					
comp	0.5020	0.5380	0.1885	0.1795	0.0899
sum	29.1	11.0	21.1	10.6	10.1
avg	18.8	2.7	7.1	2.8	7.1
srs	8.6	-5.6	-6.9	-5.0	4.0
fm	7.4	-6.5	-9.6	-5.6	4.0
fma	18.1	2.1	5.8	2.7	7.1

TABLE 1
(Continued)

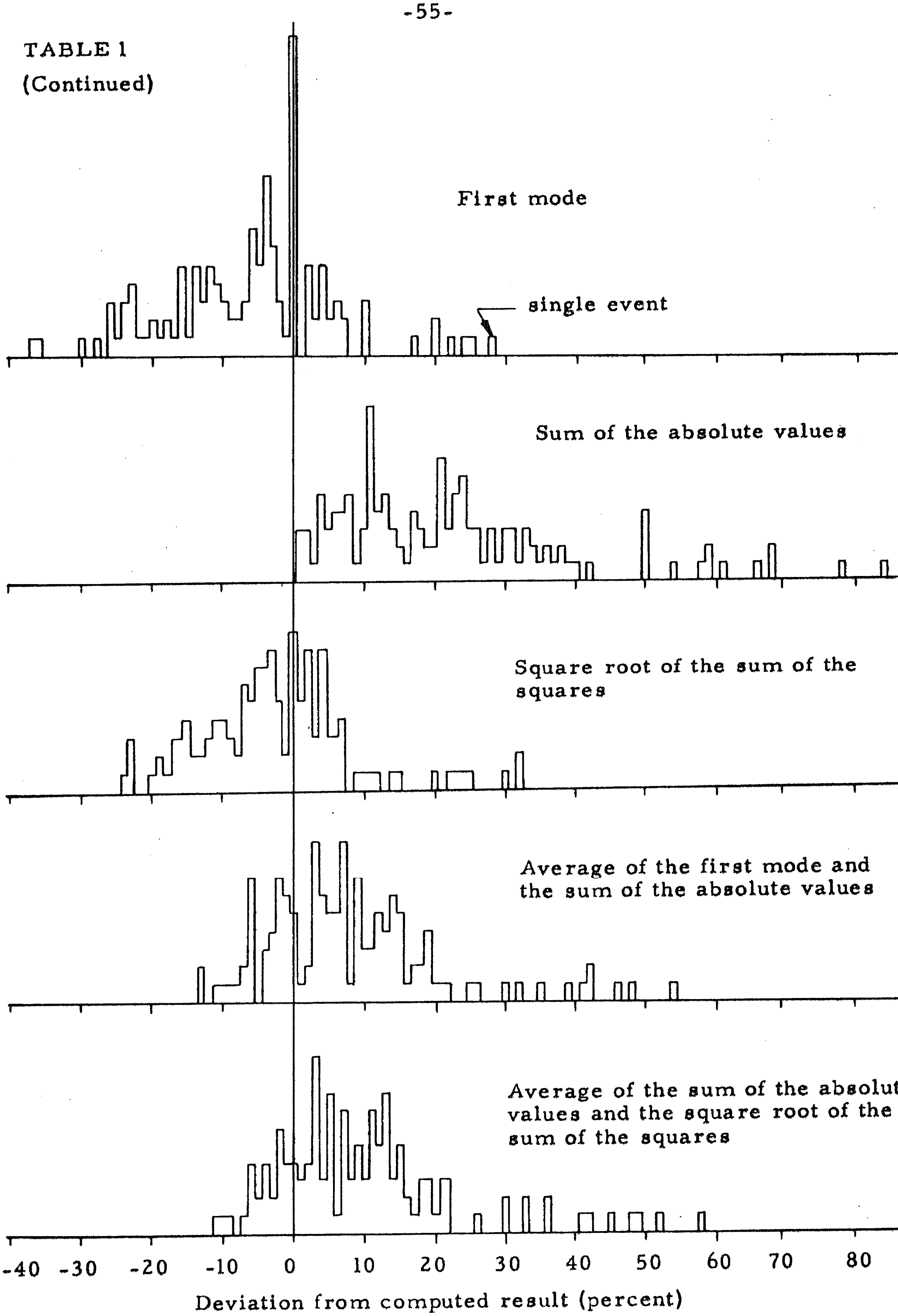

Histograms of Mode Superposition Deviations

TABLE 2

Base Moment

Values are B_M/mh

San Francisco

Damping	T (sec)	Uniform 2	Uniform 0.5	Taper 2	Taper 0.5	Step 2	Step 0.5
0, 0, 0	Computer	6.9	33.7	10	53.6	11.5	49
	1st Mode	6.9	34.5	11.25	50	12.1	49
2.5, 5, 5	Computer	6.32	22.2	9.36	36.2	9.52	32.3
	1st Mode	5.36	22.2	9.36	35	8.65	30.6
5, 5, 5	Computer	5.75	19.15	8.75	31.8	9.23	28.3
	1st Mode	5.36	19.15	9.36	31.2	8.06	27.7

Taft

Damping	T (sec)	Uniform 2.5	Uniform 1.5	Taper 2.5	Taper 1.5	Step 2.5	Step 1.5
0, 0, 0	Computer	27.9	44.6	36.4	63.6	33.6	58.9
	1st Mode	24.6	44.6	36.4	63.6	33.6	60.5
2.5, 5, 5	Computer	20.6	39	34.6	54.6	31.9	52.1
	1st Mode	22.3	39	34.6	50	32.8	50.5
5, 5, 5	Computer	18.4	33.5	36.4	47.4	28.6	46.2
	1st Mode	20.6	33.5	36.4	46.4	31.9	46.2

El Centro

Damping	T (sec)	Uniform 1.5	Taper 1.5	Step 1.5
0, 0, 0	Computer	63.8	99.8	94
	1st Mode	60.6	104	101
2.5, 5, 5	Computer	30	60.3	52.6
	1st Mode	31.9	62.3	53.6
5, 5, 5	Computer	31.9	52	46
	1st Mode	28.7	52	48

TABLE 3

Alexander Building Check

	Acceleration 16th Floor (g's)		Acceleration 11th Floor (g's)	
	Differential Analyzer	Passive Computer (24)	Differential Analyzer	Passive Computer (24)
First Mode	0.0362	0.037	0.0274	0.028
Second Mode	0.0486	0.047	0.0251	0.024
Third Mode	0.0448	0.050	0.0346	0.037
Absolute Sum	0.1296	0.134	0.0871	0.089
Square Root Sum of Squares	0.0752	0.078	0.0508	0.052
Average	0.1024		0.0689	
Computer (3 Mode approx.)	0.0819		0.0614	
Measured	0.085		0.062	

REFERENCES

1. Neumann, Frank, "A Mechanical Method of Analyzing Accelerograms," Proceedings of American Geophysical Union, Washington, D.C., (May 1-2, 1936).

2. Housner, G.W., and McCann, G.D., "The Analysis of Strong-Motion Earthquake Records with the Electric Analog Computer," Bulletin of the Seismological Society of America, Vol. 39 No. 1, (January 1949).

3. Murphy, M.J., Bycroft, G.N., and Harrison, L.W., "Electrical Analog for Earthquake Shear Stresses in a Multi-Storey Building," Proceedings of the First World Conference on Earthquake Engineering, Berkeley, California, (June, 1956).

4. Caughey, T.K., Hudson, D.E., and Powell, R.V., "The C.I.T. Mark II Electric Analog Type Response Spectrum Analyzer for Earthquake Excitation Studies," Earthquake Engineering Research Laboratory Report, California Institute of Technology, Pasadena, California, (March 1960).

5. Berg, Glenn V., "The Analysis of Structural Response to Earthquake Forces," Publication of the Industry Program of the College of Engineering, University of Michigan, Ann Arbor, Michigan, (May 1958).

6. Jennings, R.L., and Newmark, N.M., "Elastic Response of Multi-Story Shear Beam Type Structure Subjected to Strong Ground Motion," Proceedings of the Second World Conference on Earthquake Engineering, Tokyo and Kyoto, Japan, (July 1960).

7. Jennings, R. L., "The Response of Multi-Storied Structures to Strong Ground Motion," Master of Science Thesis, University of Illinois, Urbana, Illinois, (1958).

8. Stockdale, William K., "Use of Response Spectra in the Dynamic Analysis of Systems with Two Degrees of Freedom," Doctor of Philosophy Thesis, University of Illinois, Urbana, Illinois (1959).

9. Savage, J.C., "Earthquake Studies for Pit River Bridge," Civil Engineering, Vol. 9 No. 8, (August 1939).

10. Bisplinghoff, R.L., Pian, T.H., and Levy, L.I., "A Mechanical Analyzer for Computing Transient Stresses in Airplane Structure," Journal of Applied Mechanics, Vol. 17, (Sept. 1950), pp. 310-314.

11. Biot, M.A., "A Mechanical Analyzer for the Prediction of Earthquake Stresses," Bulletin of the Seismological Society of America, Vol. 31 No. 2, (April 1941).

12. Macduff, J.W., "A Pendulum Analyzer for Mechanical Transients," Proceedings of the Society for Experimental Stress Analysis, Vol. V No. 2, (1948), p. 95.

13. Rubin, Sheldon, "Response of Complex Structures from Reed-Gage Data," Journal of Applied Mechanics, Vol. 25, (Dec. 1958), pp. 501-508.

14. Biot, M.A., "Analytical and Experimental Methods in Engineering Seismology," Transactions of the American Society of Civil Engineers, Paper No. 2183, Vol. 108, (1943). (Refer to Discussion)

15. Clough, R.W., "On the Importance of Higher Modes of Vibration in the Earthquake Response of a Tall Building," Bulletin of the Seismological Society of America, Vol. 45 No. 4, (Oct. 1955) p. 289.

16. Fung, Y.C. and Barton, M.V., "Some Shock Spectra Characteristics and Uses," Journal of Applied Mechanics, Paper No. 58-APM-5, (1958).

17. Rosenblueth, Emilio, "A Basis for Aseismic Design of Structures," Doctor of Philosophy Thesis, University of Illinois, Urbana, Illinois, (1951).

18. Rosenblueth, Emilio, "Some Applications of Probability Theory in Aseismic Design," Proceedings of the First World Conference on Earthquake Engineering, Berkeley, California, (1956).

19. Goodman, L.E., Rosenblueth, E., and Newmark, N.M., "Aseismic Design of Elastic Structures Founded on Firm Ground," Proceedings American Society of Civil Engineers, Vol. 79 No. 349, (Nov. 1953).

20. Hildebrand, F.B., Methods of Applied Mathematics, New York: Prentice Hall, Inc., (1952).

21. Lord Rayleigh, Theory of Sound, New York: Dover Publications, (1945), Vol. I.

22. Caughey, T.K., "Classical Normal Modes in Damped Linear Dynamic Systems," Journal of Applied Mechanics, Paper No. 59-A-62, (1959).

23. Housner, G.W., Martel, R.R., and Alford, J.L., "Spectrum Analysis of Strong-Motion Earthquakes," Bulletin of the Seismological Society of America, Vol. 43 No. 2, (April 1953), p. 97.

24. Hudson, D.E., "Response Spectrum Techniques in Engineering Seismology," Proceedings of the First World Conference on Earthquake Engineering, Berkeley, California, (June 1956).

25. Miller, K.S., Engineering Mathematics, New York: Rinehart & Company, Inc., (1957), p. 316.

26. Stumpf, Henry J., "Response of Mechanical Systems to Random Exciting Forces", U.S. Naval Ordnance Test Station Report No. 7010 (December, 1959).

27. Blume, J.A., "Period Determination and Other Earthquake Studies of a Fifteen-Story Building," Proceedings of the First World Conference on Earthquake Engineering, Berkeley, California, (June 1956).

28. Hudson, D.E., "A Comparison of Theoretical and Experimental Determinations of Building Response to Earthquakes," Proceedings of the Second World Conference on Earthquake Engineering, Tokyo and Kyoto, Japan, (July 1960).

29. Morse, P.M., Vibrations and Sound, New York: McGraw-Hill Book Company, Inc., (1948).

30. Schlichting, Hermann, Boundary Layer Theory, New York: McGraw-Hill Book Company, Inc., (1960), Fourth Edition.

31. Housner, G.W., and Hudson, D.E., Applied Mechanics Dynamics, New York: D. Van Nostrand Company, Inc., (1959), Second Edition, p. 140.

Appendix I

Air Damping

A single degree of freedom system was selected as a numerical example (fig. I-1).

The three effects mentioned in the text were:

1. Increase in effective mass
2. Radiation of energy
3. Viscous effects.

The values assumed for the example are:

$a = 5$ (ft)

$h = 15$ (ft)

$m = \frac{4000}{32.2} \left(\frac{\text{lb sec}^2}{\text{ft}}\right)$

Velocity of Top = $V = U_o \sin \omega t$

Natural Period of System = $T_o = 0.5$ (sec)

Density of Air (NACA STD Atmosphere, Sea Level) $\rho = \frac{0.0765}{32.2} \left(\frac{\text{lb sec}^2}{\text{ft}}\right)$

Kinamatic Viscosity (NACA STD Atmosphere, Sea Level) $\nu = 1.56 \times 4 \times 10^{-4} \left(\frac{\text{ft}^2}{\text{sec}}\right)$

Speed of Sound (NACA STD Atmosphere, Sea Level) $C_s = 1117$ (ft/sec)

The first is not a dissipative effect but will be mentioned here. The effective mass is approximately equal to $(h\pi a^2 \rho + m)$ if the entire building is assumed to vibrate with the same velocity (fig. I-1c), (29).

$$M_{effective} \approx h\pi a^2 \rho + m$$

$$\approx \frac{90 + 4000}{32.2}$$

% increase = 2.25%

This would have a negligible effect on the response.

If the wavelength (λ) is long compared to the dimension of the radiating body, then the details of the shape of the body become unimportant. For the representative period 0.5 seconds

$$\lambda = T\, C_s = 558.5 \text{ (ft)}$$

The characteristic dimension in this case would be 2a (10 feet). Therefore, since the particular shape is unimportant, a cylinder was chosen and uniform vibration of the entire body was again assumed (fig. I-1b). Energy radiated per unit time from a cylinder moving with velocity $U_o \sin \omega t$ neglecting end effects is (29)

$$E_{\text{radiation/unit time}} = \frac{\pi^2 \omega^3 \rho\, a^4 U_o^{\,2} h}{4 C_s^{\,2}} \tag{I-1}$$

The viscous effect was estimated by considering the energy lost in the boundary layer on the sides and top of the structure parallel to the motion. The entire body was again assumed to move at the same velocity (fig. I-1c). The velocity profile on a flat plate oscillating with velocity $U_o \sin \omega t$, neglecting edge effects, and assuming a viscous, incompressible fluid with a laminar boundary layer is (30)

$$U(y, t) = U_o e^{-\sqrt{\frac{\omega}{2\nu}}} \sin\left(\omega t - \sqrt{\frac{\omega}{2\nu}}\; y\right) \tag{I-2}$$

where y is measured perpendicular to the plate.

$$\text{Shear at wall} = \nu \rho \left(\frac{\partial U}{\partial y}\right)_{y=0}$$

$$E_{\text{viscous}} \Big/ \begin{array}{l}\text{unit}\\ \text{time}\end{array} = \frac{U_o^{\,2} h a \not{\phi} \sqrt{\nu}}{\sqrt{2\omega}} \tag{I-3}$$

For a single degree of freedom system with internal viscous damping and vibrating with velocity $U_o \sin \omega t$, the energy dissipated is (31):

$$E_{\substack{\text{viscous}\\ \text{dashpot}}} \Big/ \begin{array}{l}\text{unit}\\ \text{time}\end{array} = \rho \omega_o m U_o^{\,2} \tag{I-4}$$

where ρ is the damping ratio $C/C_{critical}$.

An effective damping ratio (ρ_{eff}) may be calculated by equating the energy obtained from equations I-1 and I-3 to that from I-4 and solving for ρ.

$$\rho_{eff} = \frac{\pi^2 \omega^3 \not{\phi} a^4 h}{4 C_s^{\,2} \omega_o m} + \frac{h a \not{\phi} \sqrt{\nu}}{\sqrt{2\omega}\, \omega_o m}$$

evaluate at resonance, $\omega = \omega_o$

$$\rho_{eff} = 5.60 \times 10^{-5} + 2.84 \times 10^{-7}$$

$$\rho_{eff} = 562.8 \times 10^{-7}$$

In the usual case the damping ratio in a building is of the order of 0.01 to 0.1 and therefore the above effects would be negligible.

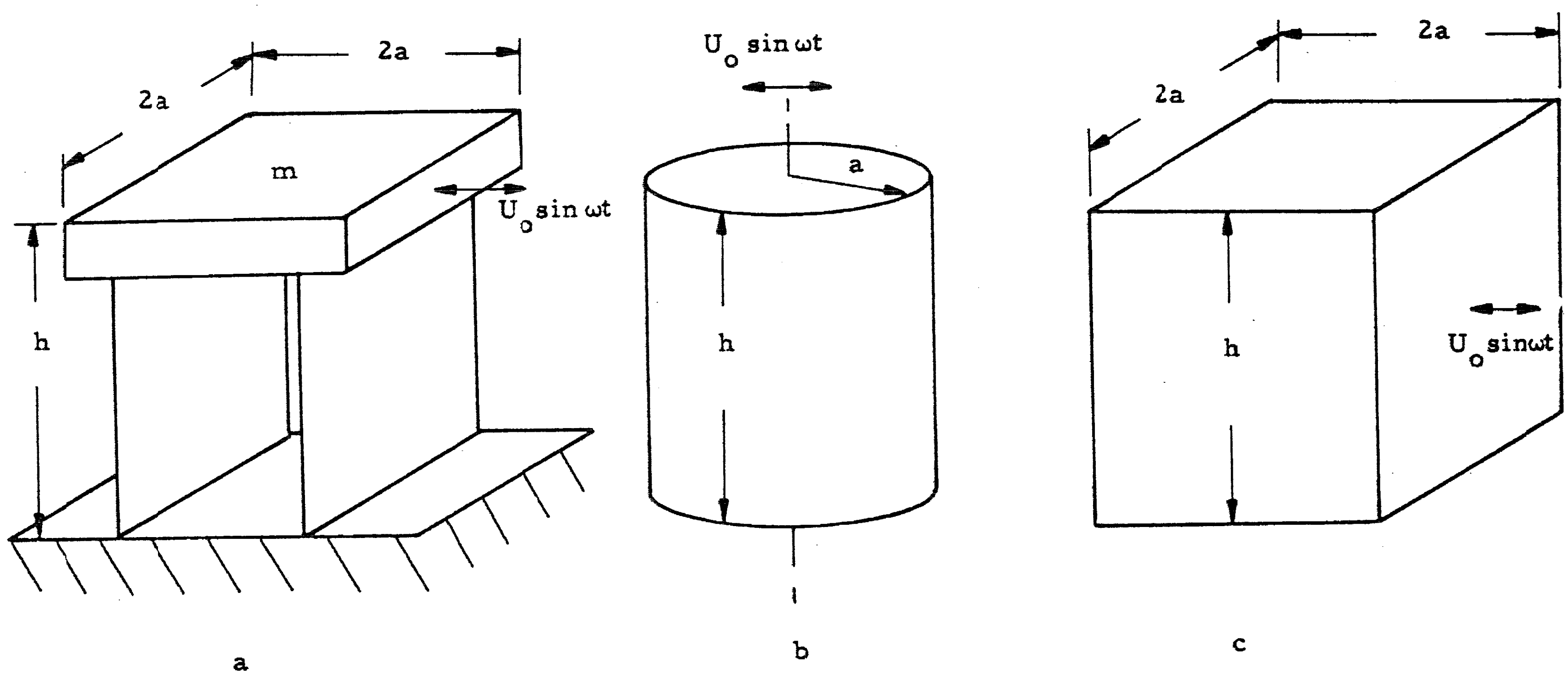

Figure I-1
Air Damping Model

Appendix II

Distribution of Local Maxima and Minima of Typical Earthquake Accelerograms

One significant property of a complicated function such as an earthquake accelerogram is the probability distribution of the accelerations. To investigate these distributions for actual earthquakes, four typical accelerograms were chosen.

The earthquake accelerogram has three sections -- a leading section of low amplitude and rapid variation, a central section which is the body of the tremor, and a terminal section of relatively low amplitude and slow variation. For the purposes of a statistical distribution study the central section alone is of concern. Values may be obtained by reading accelerations at equal time intervals or by reading values at random points along the accelerogram. Since the accelerogram changes so rapidly, resulting in nearly vertical segments, both of these methods lead to difficulty in obtaining accurate readings. Consequently, readings were taken at every point of abrupt change in slope. Since this includes all of the peaks along the accelerogram it is doubtful if this is truly a random selection and would better be described as the distribution of local maxima and minima. The readings were converted to the same scale and plotted together on normal probability paper in figure II-1. A straight line on such a plot is a Gaussian distribution with slope a function of the variance.

The sample treated here is not large enough to allow a positive statement concerning the distribution. The experimental work of the present thesis does not require hypotheses as to probability distribution, but the data has been included because of its possible interest for future extensions of the theory.

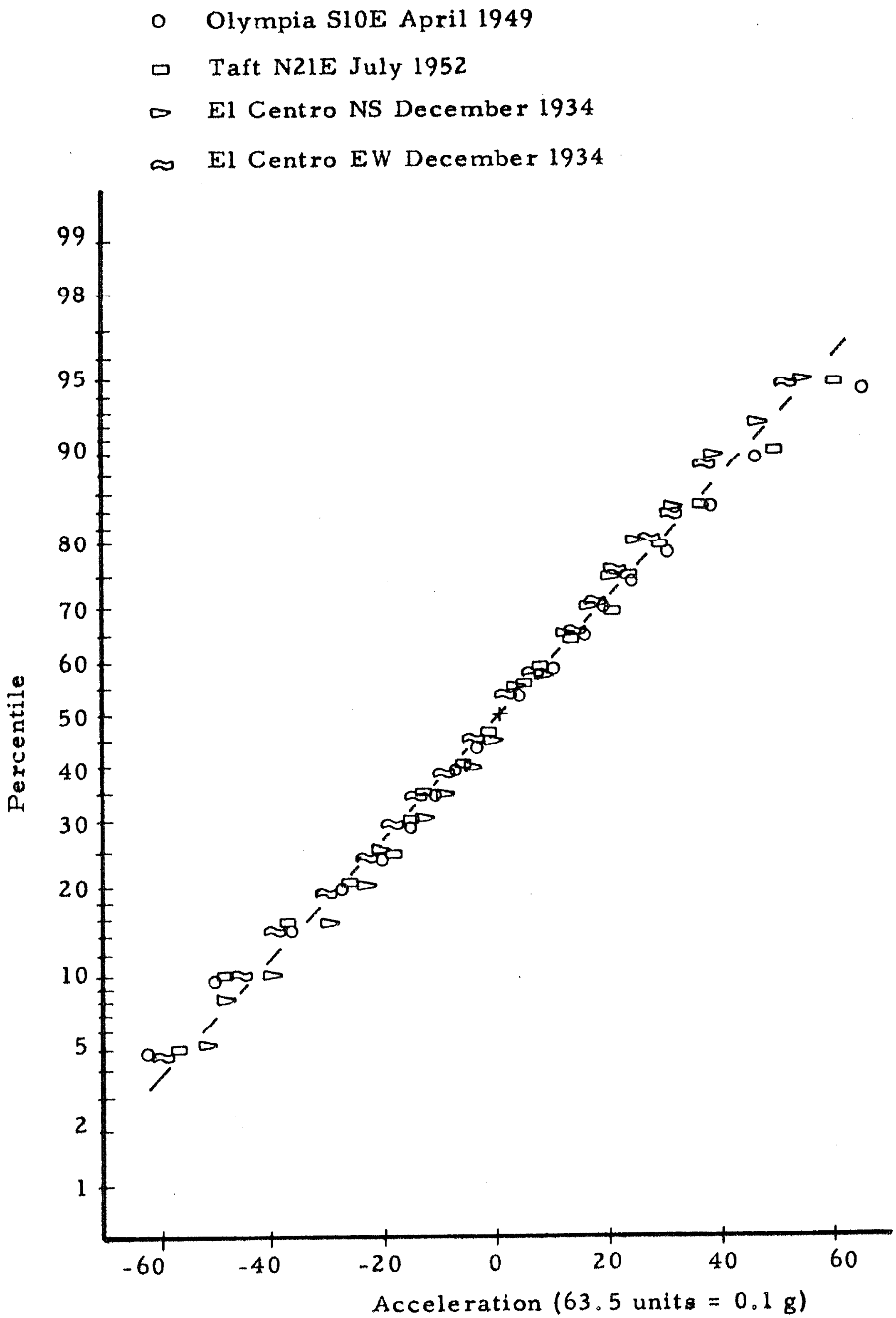

Figure II-1

Distribution of Local Maxima and Minima of Typical Earthquake Accelerograms.

Appendix III

Experimental Setup

The differential analyzer used for the experimental work was designed to solve equation 51 for each mode.

$$\ddot{\xi}_{si} = -2\rho\omega_i \dot{\xi}_{si} - \omega_i^2 \xi_{si} + \ddot{y}(t)$$

The equation was solved by integrating the acceleration $\ddot{\xi}_{si}$ twice (fig. III-3), $\ddot{\xi}_{si}$ being obtained by summing the proper feedbacks and inputs (fig. III-4 and III-2). The basic requirements are a velocity feedback to the mode summer to obtain the positive damping term $(2\rho_i\omega_i \dot{\xi}_{si})$ and a displacement feedback to obtain the proper natural frequency $(\omega_i^2 \xi_{si})$. The negative damping feedback was included to obtain the zero damping case, the feedback compensating for any losses in the system.

The earthquake input $\ddot{y}(t)$ was repeated ten times per second by means of a circular, variable width film and a photoelectric reader (4). The residual oscillations in each mode must be damped out after each repetition to prevent interference. This was the function of the damping pulse arrangement (fig. III-8). To obtain sufficient damping in all cases it was found necessary to multiply the feedback to the mode summer by five in each mode.

The frequency feedback was adjusted by switching the input (fig. III-2) to a sine wave generator set to the desired frequency and visually peaking the system response by adjusting the feedback potentiometer. The response may be observed on the oscilloscope but a RMS voltmeter was found more convenient. The negative damping was set by applying a pulse to the system at 10 cps and adjusting the negative damping potentiometer, with positive damping on zero, until the envelope was neither decreasing nor increasing. The pulse was obtained by biasing the last integrator off zero, with no input, thus allowing the damping pulse arrangement to give a sharp pulse at 10 cps.

The amplifiers were then all properly biased and the damping set to the desired value. By proper switching it was possible to obtain any combination of any of the modes reading either displacement, velocity, or relative or absolute acceleration, or any mode response individually (spectrum point).

The combining coefficient $Q_{ij} G_j$ of equation 52 was set with the 1/10 factor potentiometer of each mode (fig. III-5) and the sign was entered in the combination summer (fig. III-9).

For stability all the equipment was driven from constant voltage transformers and a low pass filter (fig. III-7, less than 10 cps for any attenuator setting of interest) was used in the input to prevent D.C. drift.

If absolute damping is being considered the $\dot{y}(t)$ can be obtained by integrating the input once. Since there is no direct feedback for an integrator used in this way, a small resistive feedback is introduced for stability (fig. III-6). The coefficient again can be set by means of a potentiometer.

In all that has been said above it has been assumed that $\ddot{y}(t)$ is introduced in real time and the multiplicative factors introduced by the various integrators have been ignored.

The time scale is changed due to the function generator:

$$t_r = Nt_a \qquad \text{(III-1)}$$

where

t_r = real time

t_a = analog time

$$N = \frac{\text{(actual time duration of record) sec}}{\left(\dfrac{\text{number of degrees of disk required for record}}{360}\right)\dfrac{\text{degrees}}{\text{rev}}\left(\dfrac{1}{10}\right)\dfrac{\text{sec}}{\text{rev}}}$$

since the variable width film revolves at 10 cps. Also it follows that $\omega_a = N\omega_p$. If a peak on the original record is r g's and the same peak reproduced by the function generator is ℓ, divisions of the oscilloscope face, then

$$\begin{aligned} Z_r &= N^2 V_a \frac{r\,32.2}{\ell} \\ \dot{Z}_r &= N \dot{V}_a \frac{r\,32.2}{\ell} \\ \ddot{Z}_r &= \ddot{V}_a \frac{r\,32.2}{\ell} \end{aligned} \qquad \text{(III-2)}$$

where the Z_r are real responses in feet and seconds and V_a are the analog responses in lines of the oscilloscope face.

The output of each integrator in the modes is 1/RC times the integrated input. Letting primes refer to the second integrator in each mode and taking into account equations III-2 the following equations are obtained:

Displacement spectrum ith mode (ft)

$$\xi_{si} = \left(\frac{r}{\ell}\,32.2N^2 C_i R_i C_i' R_i'\right) \xi_{ai} \qquad \text{(III-3)}$$

Velocity spectrum (ft/sec)

$$\dot{\xi}_{si} = \left(\frac{r}{\ell}\,32.2N\,C_i' R_i'\right) \dot{\xi}_{ai} \qquad \text{(III-4)}$$

Acceleration spectrum (ft/sec^2) relative

$$\ddot{\xi}_{si} = \left(\frac{r}{\ell}\, 32.2\right) \ddot{\xi}_{ai} \tag{III-5}$$

Acceleration spectrum (ft/sec^2) absolute

$$\bar{\ddot{\xi}}_{si} = \left(\frac{r}{\ell}\, 32.2\right) \ddot{\xi}_{ai} - \ddot{y}) = \left(\frac{r}{\ell}\, 32.2\right) \bar{\ddot{\xi}}_{ai} \tag{III-6}$$

The minus sign of $\ddot{y}$ is due to the convention that correct signs for $\bar{\ddot{\xi}}_{ai}$ are only obtained when multiplied by the proper G_i. Displacement of ith floor in actual system (ft)

$$x_i = \frac{r}{\ell}\; 32.2N^2 \sum_{j=1}^{3} Q_{ij} G_j C_j R_j C_j' R_j' \; \xi_{aj} \tag{III-7}$$

Relative displacement of ith and kth floor (ft)

$$x_i - x_k = \frac{r}{\ell}\, 32.2N^2 \sum_{j=1}^{3} G_j C_j R_j C_j' R_j' (Q_{ij} - Q_{kj}) \; \xi_{aj} \tag{III-8}$$

Velocity of ith floor (ft/sec)

$$\dot{x}_i = \frac{r}{\ell}\, 32.2N \sum_{j=1}^{3} Q_{ij} G_j C_j' R_j' \; \dot{\xi}_{aj} \tag{III-9}$$

Relative velocity of ith and kth floor (ft/sec)

$$\dot{x}_i - \dot{x}_k = \frac{r}{\ell}\, 32.2N \sum_{j=1}^{3} G_j C_j' R_j' (Q_{ij} - Q_{kj}) \; \dot{\xi}_{aj} \tag{III-10}$$

Absolute acceleration (ft/sec^2)

$$\bar{\ddot{x}}_i = \frac{r}{\ell}\, 32.2 \left(\sum_{j=1}^{3} Q_{ij} G_j \; \ddot{\xi}_{aj} + \ddot{y} \right) \tag{III-11}$$

Base moment (lb ft)

$$M_B = \sum_{j=1}^{3} m_j \ddot{x}_j k_j \qquad \text{(III-12)}$$

where $\ddot{x}_j$ is given by equation III-11.

In the above equations the ξ_i's and x_i's are maxima in the units stated and the ξ_{ai}'s are the maxima read from the oscilloscope in equations III-3 to III-5. The combinations given in equations III-6 to III-12 are made to within a constant factor by the computer and the maxima of this read from the oscilloscope. These values will be referred to in the data compilations as x_{ai}'s.

Errors involved in the analog results are from two sources, machine inaccuracies and human error.

All the resistors required in the setup had 1% tolerance. By proper selection and combination the capacitive elements were within less than 1.5% of the desired value. Calibration charts were prepared for all potentiometers that had to be set to a specific numerical value. As mentioned before, a means was provided to allow negative feedback to be introduced and positive damping was then set from the known zero damped case. A calibration chart was also provided, for the sine wave oscillator used to set the natural frequency, by using an electronic counter.

The errors mentioned above may have little or no effect, depending on the frequency range and the damping involved. Increasing damping tends to decrease the effect of element errors, which is fortunate since the damped cases have the most importance for practical problems.

Phase shift through the mode elements was checked in the range of interest using a sine wave input and comparing this with voltages at various points in the system. The Lissajous figures resulting indicated negligible phase shift.

The major portion of the work was concerned with comparing various quantities obtained by different methods. The data used for each comparison was obtained without changing the basic setting of the analog. Therefore, the conclusions reached are relatively uneffected by machine type error.

The major source of error arises in the reading of the amplitude from the oscilloscope. The error is of the order of 5%, depending on the size of the trace in relation to the oscilloscope face. Since other errors are usually negligible by comparison, the total error would be of the order of 5%.

For checking specific cases such as the Alexander Building, definite quantities are desired. To check the accuracy of the computer for this situation, velocity spectrum values were compared to those obtained from a passive spectrum analyzer. The values are in good agreement (fig. III-10). The accuracy of the method is further borne out by a two degree of freedom test case. A resonance curve (4% damping in each mode) was obtained by a passive analog, by the first two modes of the analyzer used for this work, and exactly by using a desk calculator. The results are given in figure III-11. As can be seen, the differential analyzer gives good results and is not prone to slight shifts in resonance peaks resulting from element inaccuracies as in the passive case since the natural frequencies are set in correctly using the sine wave oscillator.

From the above it would seem proper to say that the differential analyzer type of computer used in this work is at least as accurate as the spectrum data to which any results and conclusions obtained in this thesis will be applied.

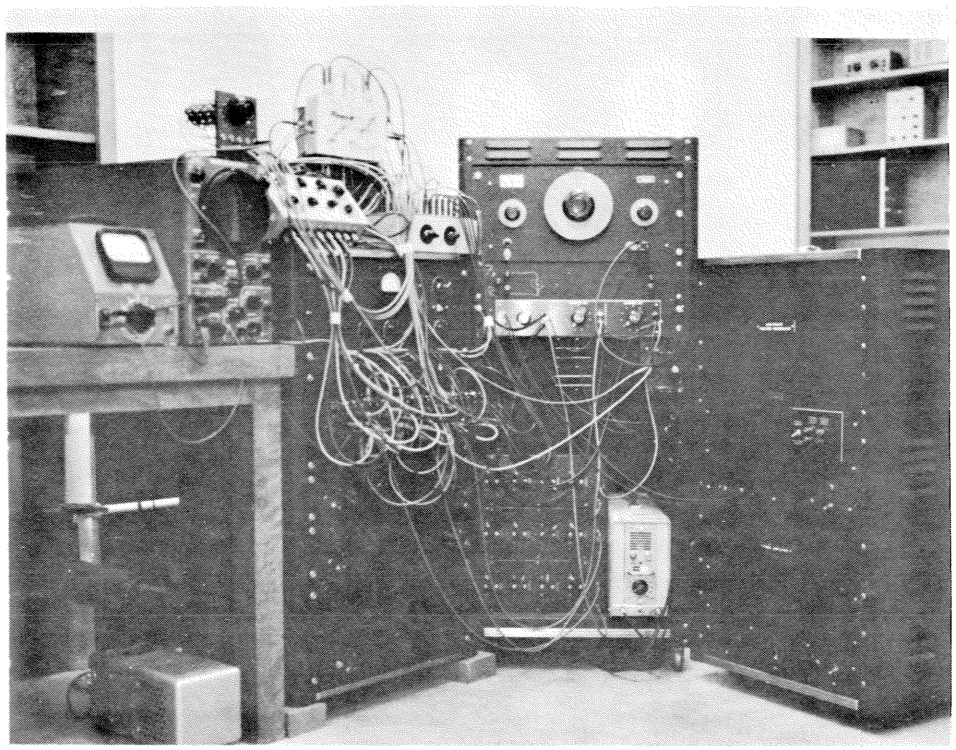

Special purpose electronic differential analyzer for a three degree of freedom system.

Figure III-1
Experimental Setup

Symbols used in this appendix are as follows:

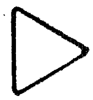	Amplifier
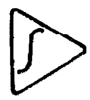	Integrating Network
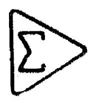	Summing Network
	Ground
	Resistance
	Variable Resistance
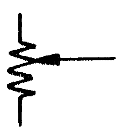	Potentiometer
	Capacitance
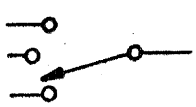	Switch

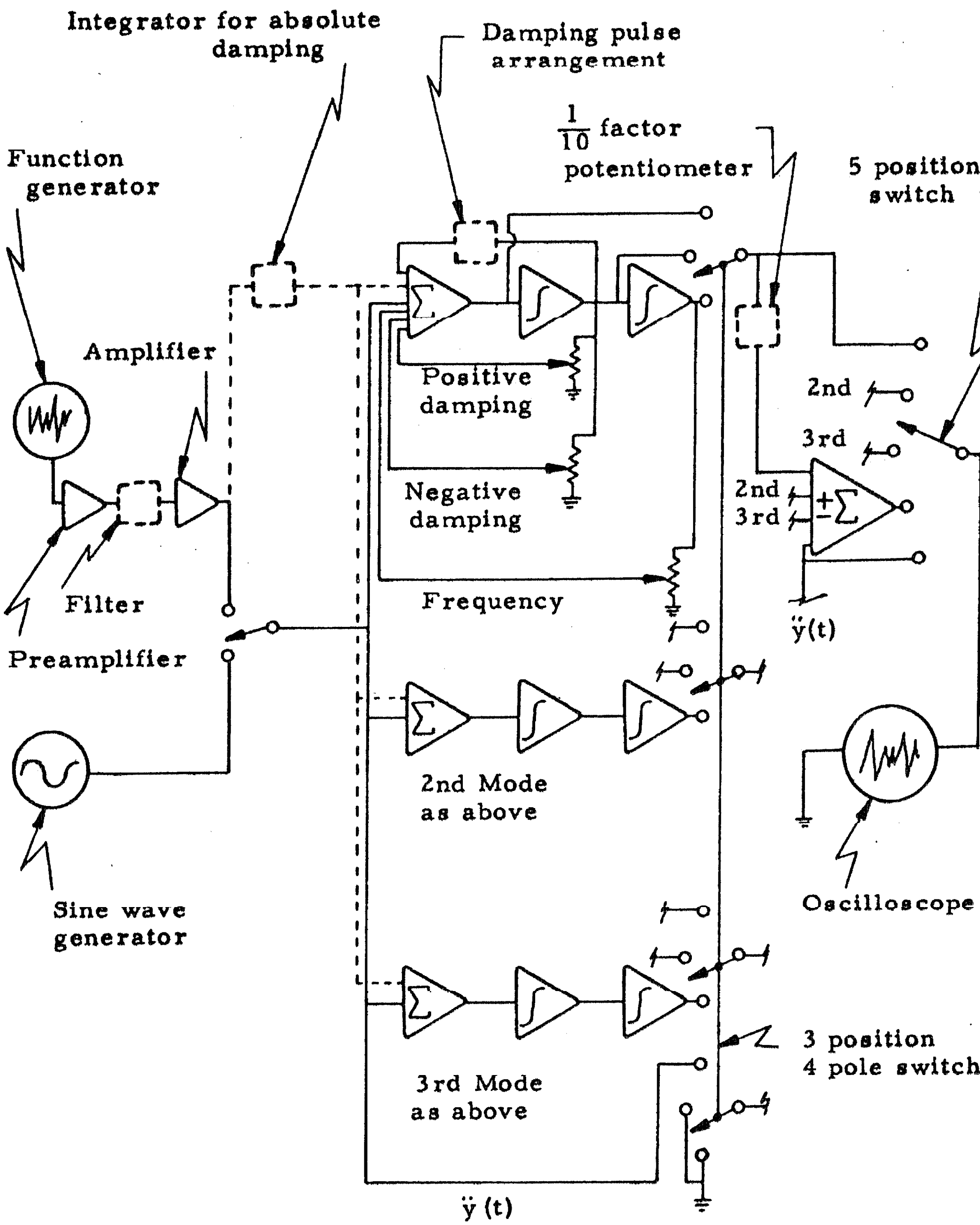

Figure III-2
Overall Diagram

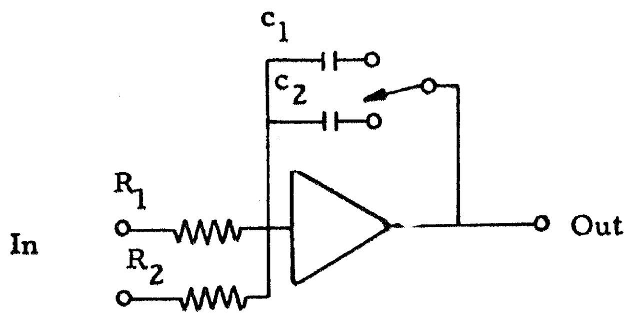

$R_1 = 10^6\,\Omega$ $\quad$ $c_1 = 0.0004\ \mu\mathrm{Fd}$

$R_2 = 10^4\,\Omega$ $\quad$ $c_2 = 0.004\ \mu\mathrm{Fd}$

$$e_{out} = -\frac{1}{RC}\int e_{in}\,dt$$

Figure III-3
Mode Integrator

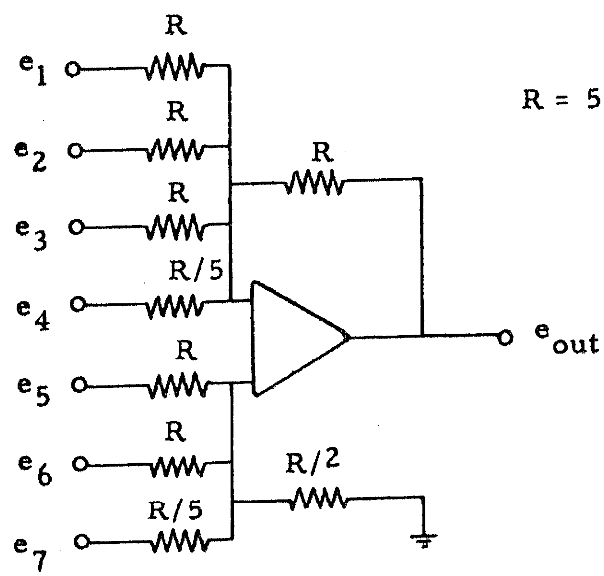

$R = 500\,\mathrm{K}\Omega$

$$e_{out} = -e_1 - e_2 - e_3 - 5e_4 + e_5 + e_6 + 5e_7$$

Figure III-4
Mode Summer

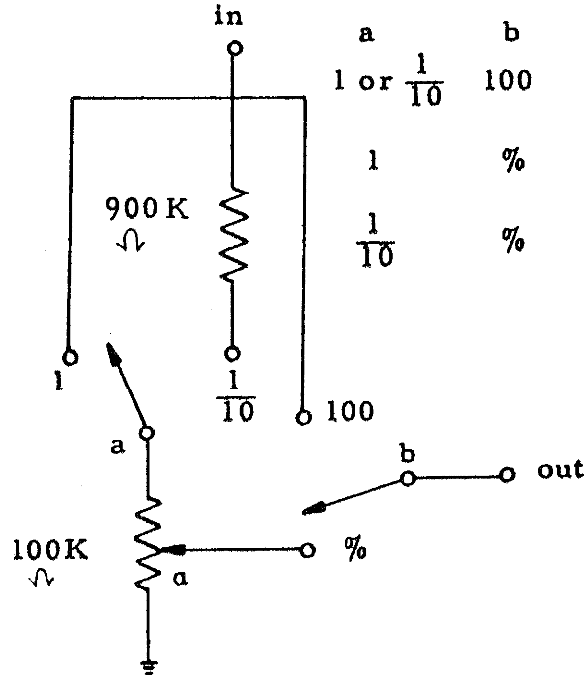

Switch a	Switch b	$\frac{out}{in}$
1 or $\frac{1}{10}$	100	1
1	%	a
$\frac{1}{10}$	%	$\frac{a}{10}$

Figure III-5

$\frac{1}{10}$ Factor Potentiometer

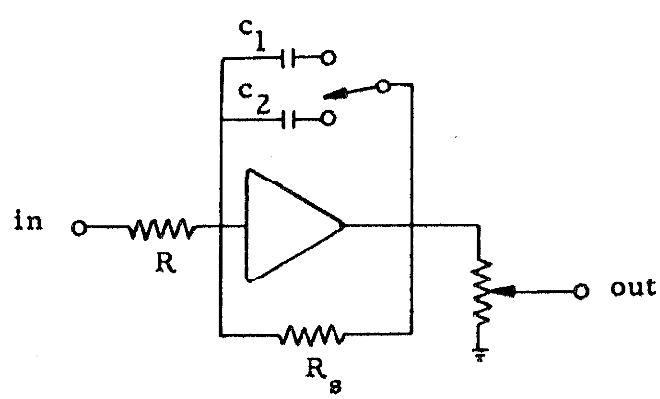

$R = 10^6 \Omega$ $\qquad$ $c_1 = 0.0004\ \mu Fd$

$R_s = 120\ M\Omega$ $\qquad$ $c_2 = 0.004\ \mu Fd$

$$e_{out} \cong - \frac{1}{RC} \int e_{in} dt$$

Figure III-6

Integrator for Inertial Damping

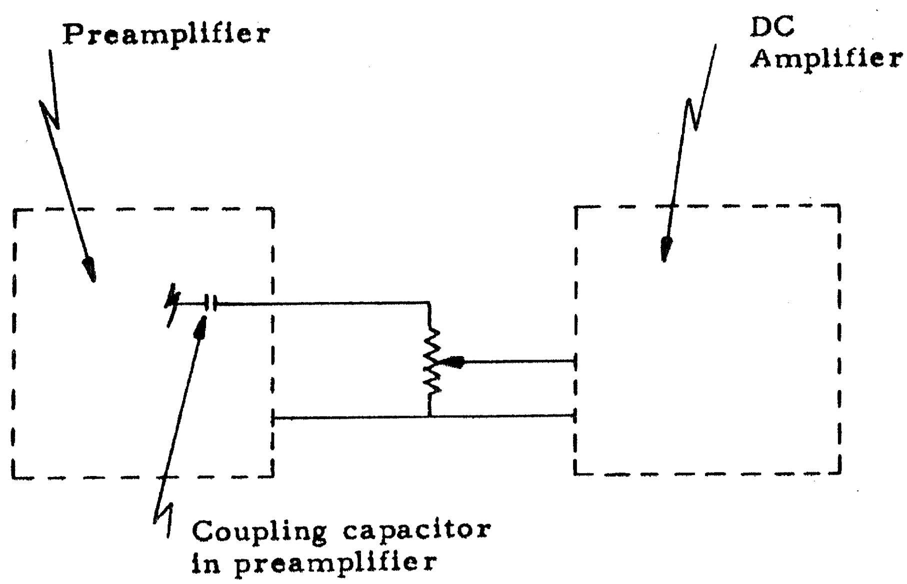

Figure III-7
Input Filter

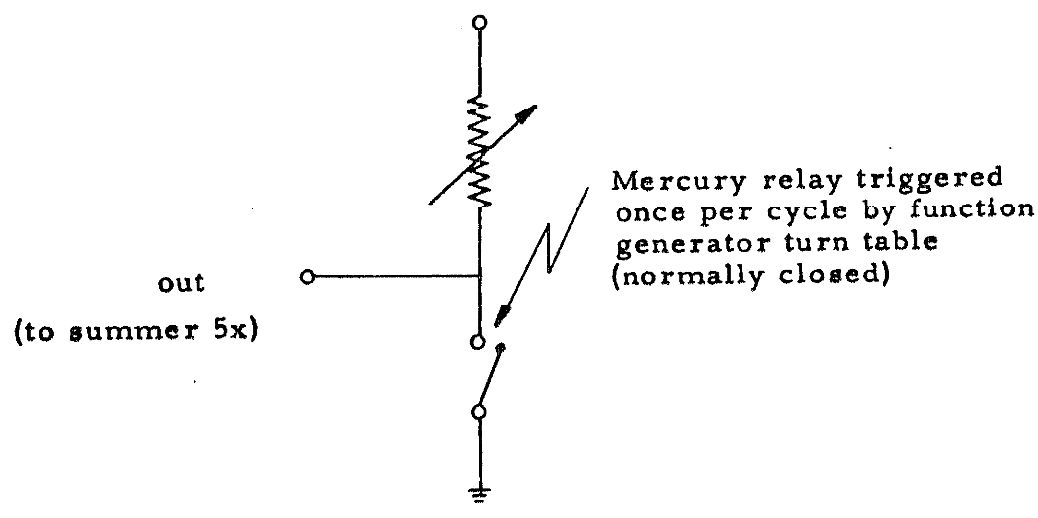

Figure III-8
Damping Arrangement

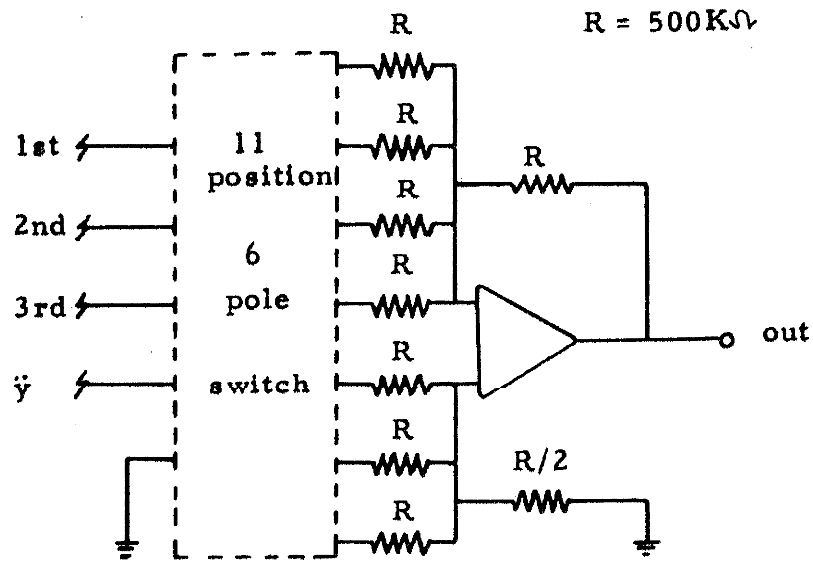

The switch allows any sign relationship of 3 or 4 inputs and the combination of any one input and ÿ to obtain the absolute acceleration spectrum points. (The ground input is provided to ground any unused input to the summer.)

Figure III-9

Combination Summer

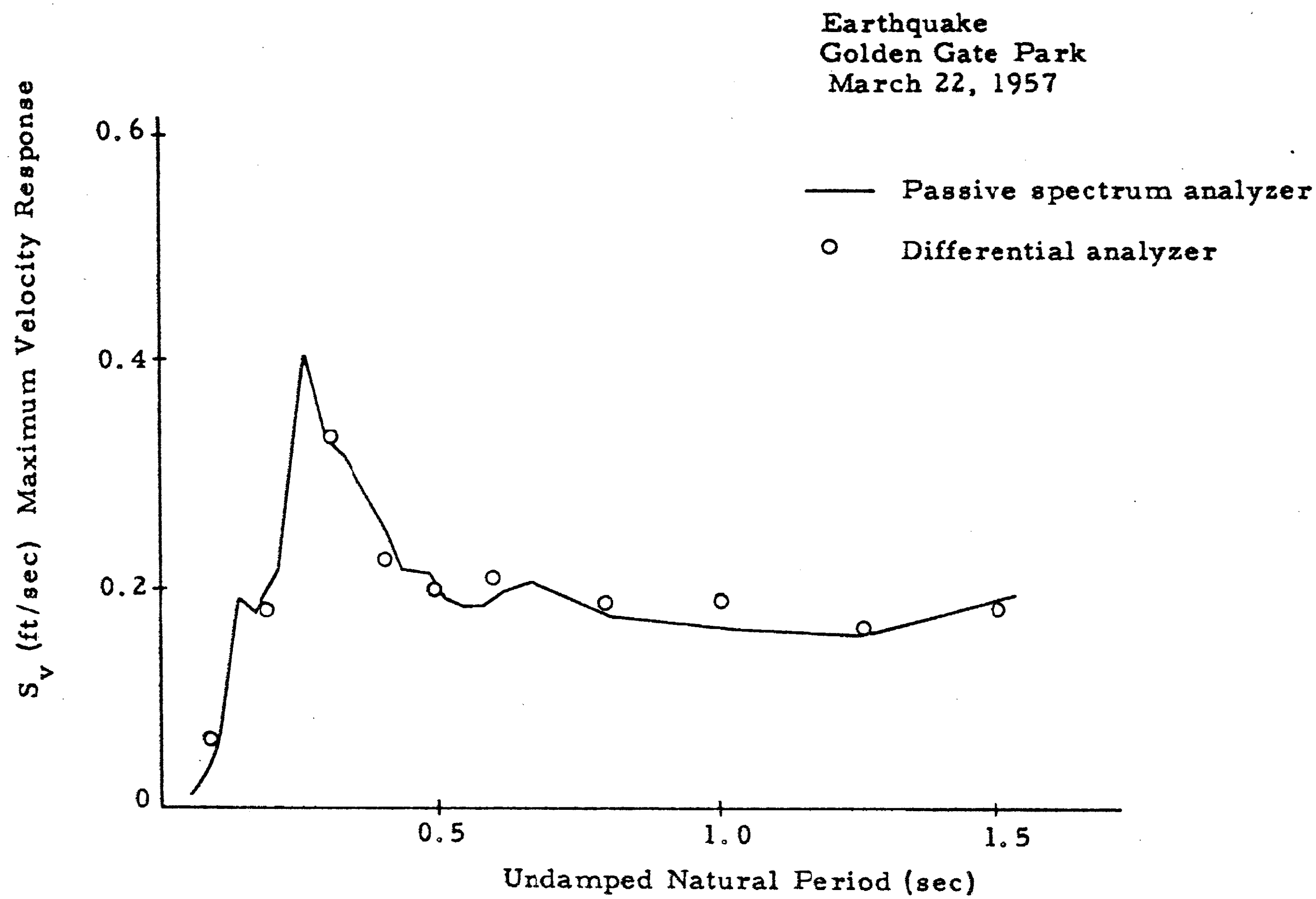

Figure III-10
Velocity Spectrum Check

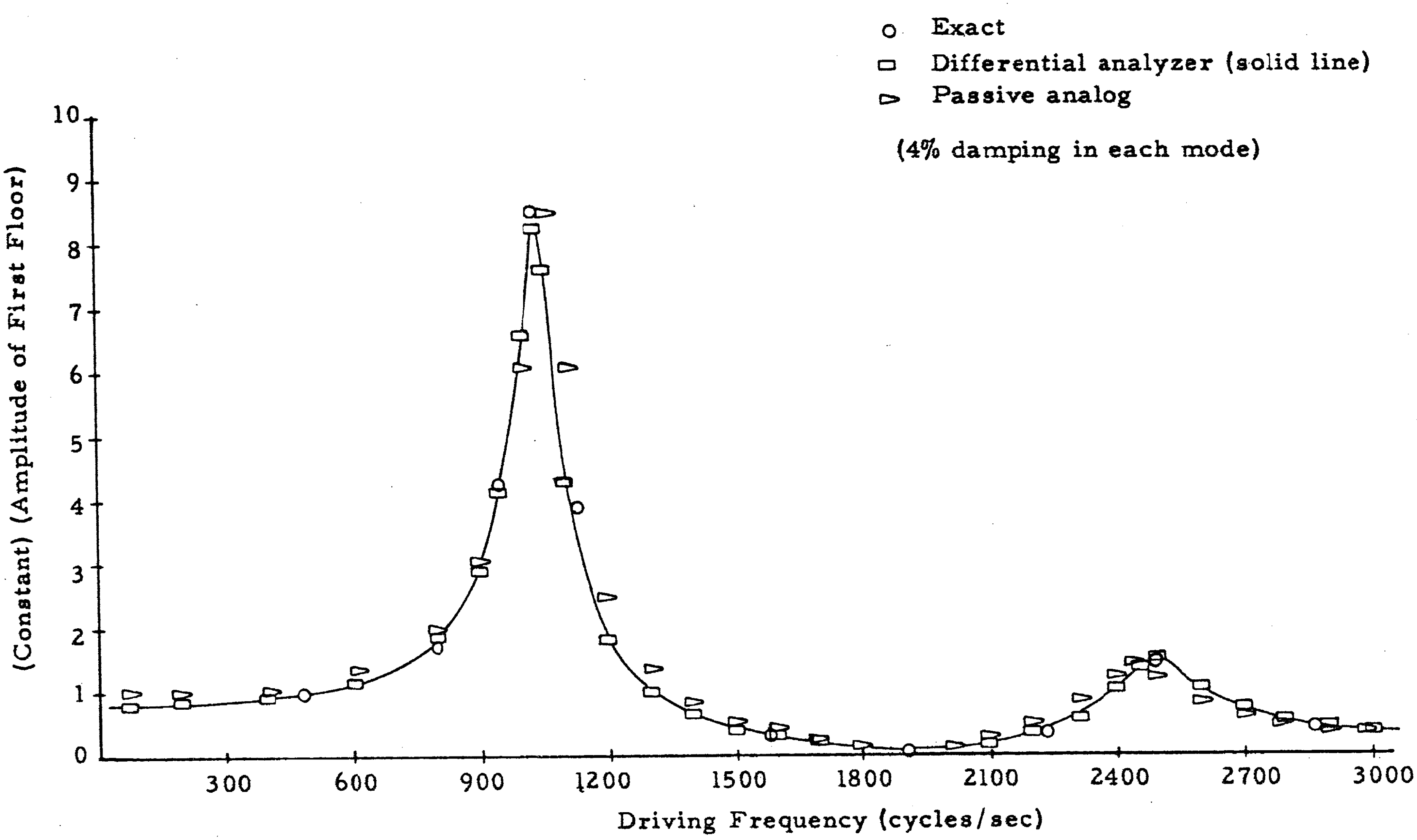

Figure III-11
Two Degree of Freedom Check

Appendix IV

Reference Data

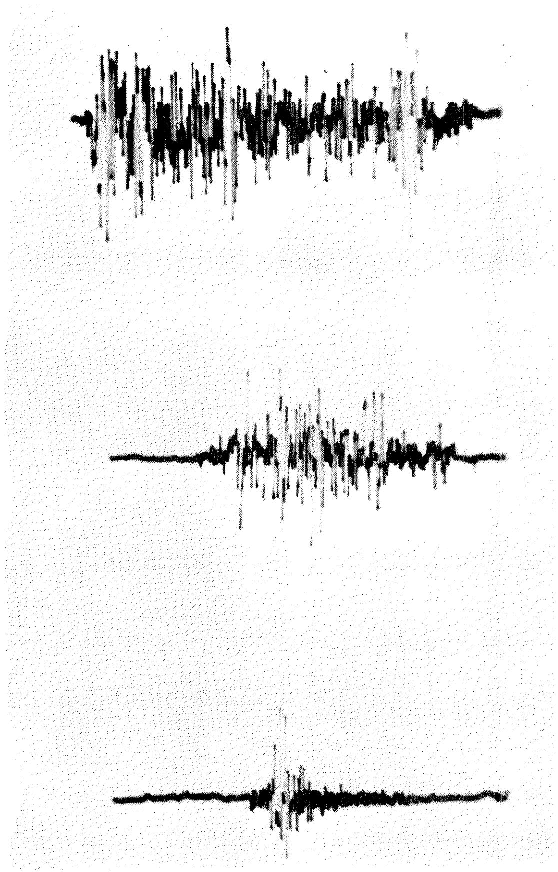

Top, El Centro
Center, Taft
Bottom, San Francisco

Figure IV-1

Accelerograms

Building Models

Uniform

$$[Q] = \begin{bmatrix} 1 & 1 & 1 \\ 0.802 & -0.555 & -2.247 \\ 0.445 & -1.245 & 1.800 \end{bmatrix}$$

$G_1 = -1.22 \qquad G_2 = 0.280 \qquad G_3 = -0.0595$

$$\omega_1 = \frac{\omega_2}{2.8} = \frac{\omega_3}{4.05}$$

Taper

$$[Q] = \begin{bmatrix} 1 & 1 & 1 \\ 0.7022 & -0.3045 & -1.5647 \\ 0.3420 & -0.5606 & 1.1616 \end{bmatrix}$$

$G_1 = -1.4678 \qquad G_2 = 0.6065 \qquad G_3 = -0.1363$

$$\omega_1 = \frac{\omega_2}{2.09} = \frac{\omega_3}{2.93}$$

Step

$$[Q] = \begin{bmatrix} 1 & 1 & 1 \\ 0.7446 & -0.3554 & -1.8892 \\ 0.4268 & -0.5514 & 2.1246 \end{bmatrix}$$

$G_1 = -1.3516 \qquad G_2 = 0.4373 \qquad G_3 = -0.0857$

$$\omega_1 = \frac{\omega_2}{2.30} = \frac{\omega_3}{3.36}$$

Alexander Building

Mode Shapes

1st	2nd	3rd
2.22	-3.48	1.90
2.10	-2.10	0
2.02	-1.00	-0.95
1.92	0.30	-1.40
1.80	1.08	-1.50
1.68	1.80	-1.40
1.50	2.10	-1.20
1.38	2.35	-0.85
1.20	2.45	-0.30
1.05	2.32	0.55
0.90	2.10	1.05
0.75	1.80	1.40
0.55	1.40	1.50
0.38	1.00	1.35
0.20	0.70	0.90

Mode	Natural Period (sec)	Damping (% critical)
1	1.27	2
2	0.41	4
3	0.24	4

$G_1 = 0.604$ $G_2 = 0.169$ $G_3 = 0.181$

Earthquake for which responses were obtained:

San Francisco (Alexander Building) N 9 W March 22, 1957
(N = 192)

Jenning 8 Story Building

Mode Shapes

1st	2nd	3rd
0.53184	0.59442	0.53898
0.49269	0.32228	-0.03810
0.43386	-0.00171	-0.47513
0.36444	-0.26035	-0.39779
0.28982	-0.40139	-0.04409
0.21367	-0.41727	0.28840
0.13868	-0.32968	0.40107
0.06692	-0.17635	0.26791

Natural frequencies (cycles/sec)

1st	0.94851
2nd	2.36546
3rd	3.77090

$G_1 = 2.64878$ $G_2 = -1.048676$ $G_3 = 0.66883$

Spring constant of lowest level

2000 Kips/in

Earthquake for which response was obtained:

El Centro EW May 18, 1940 (N = 416)

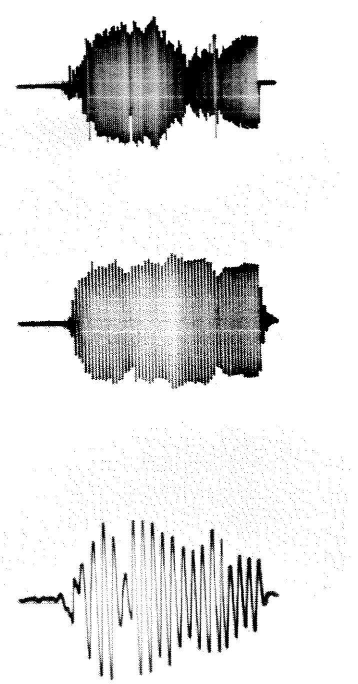

Top, 3rd Mode
Center, 2nd Mode
Bottom, 1st Mode

Figure IV-2

Typical Displacement Responses

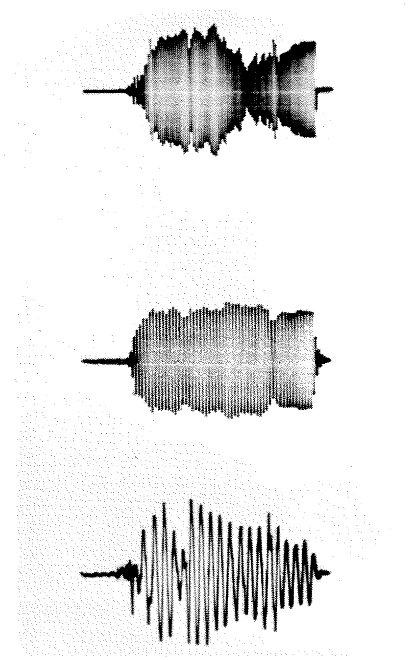

Top, 3rd Mode
Center, 2nd Mode
Bottom, 1st Mode

Figure IV-3

Typical Velocity Responses

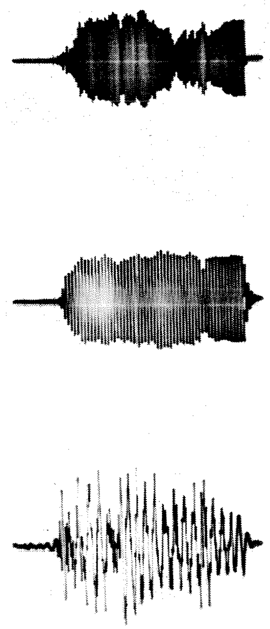

Top, 3rd Mode
Center, 2nd Mode
Bottom, 1st Mode

Figure IV-4

Typical Acceleration Responses

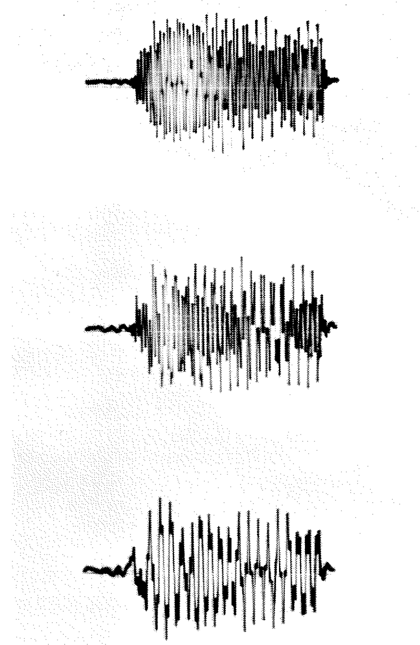

Top, Acceleration from Fig. IV-4
Center, Velocity from Fig. IV-3
Bottom, displacement from Fig. IV-2

Figure IV-5

Typical Mode Addition

General Data Conversion

The coefficients for the conversion of the spectra data in the following tables are given in equations III-3 to III-6.

For the computer summed data the following apply:

Displacements of ith floor (ft)

$$x_i = \left(\frac{m}{\ell} 32.2\, N^2\, Q_{i1} G_1 C_1 R_1 C_1' R_1'\right) x_{ai} \qquad \text{(IV-1)}$$

Velocity (ft/sec)

$$\dot{x}_i = \left(\frac{m}{\ell} 32.2\, N\, Q_{i1} G_1 C_1' R_1'\right) \dot{x}_{ai} \qquad \text{(IV-2)}$$

Relative displacement (ft)

$$x_2 - x_1 = \frac{m}{\ell} \frac{32.2}{0.9} N^2 G_2 C_1 R_1 C_1' R_1' (Q_{22} - Q_{12})(x_{a2} - x_{a1})$$

$$x_3 - x_2 = \frac{m}{\ell} 32.2\, N^2 G_1 C_1 R_1 C_1' R_1' (Q_{31} - Q_{21})(x_{a3} - x_{a2}) \qquad \text{(IV-3)}$$

Relative velocity (ft/sec)

$$\dot{x}_2 - \dot{x}_1 = \frac{m}{\ell} \frac{32.2}{0.9} N G_2 C_1' R_1' (Q_{22} - Q_{12})(\dot{x}_{a2} - \dot{x}_{a1})$$

$$\dot{x}_3 - \dot{x}_2 = \frac{m}{\ell} 32.2\, N\, G_1 C_1' R_1' (Q_{31} - Q_{21})(\dot{x}_{a3} - \dot{x}_{a2}) \qquad \text{(IV-4)}$$

Absolute acceleration

$$\ddot{x}_1 = \frac{m}{\ell} 32.2 \quad Q_{11} G_1\, \ddot{x}_{a1}$$

$$\ddot{x}_2 = \frac{m}{\ell} 32.2 \quad Q_{21} G_1\, \ddot{x}_{a2} \qquad \text{(IV-5)}$$

$$\ddot{x}_3 = \frac{m}{\ell} 32.2 \quad \ddot{x}_{a3}$$

In the above equations the x_{ai}'s are oscilloscope readings in lines. All the readings have been adjusted (by factors of 10) so that the values for capacitances and resistances are:

$$C_i = 0.004\ \mu\mathrm{Fd}$$

$$C_i' = 0.0004\ \mu\mathrm{Fd}$$

$$R_i = 10^4\ \Omega$$

$$R_i' = 10^6\ \Omega$$

Note that the spectrum values for the 2.5, 5, 5% case for the ξ_{a2}'s and ξ_{a3}'s are obtained from the values of the 5, 5, 5% case.

San Francisco
Uniform

T_1	ξ_{a1}	ξ_{a2}	ξ_{a3}	$\dot{\xi}_{a1}$	$\dot{\xi}_{a2}$	$\dot{\xi}_{a3}$	$\ddot{\xi}_{a1}$	$\ddot{\xi}_{a2}$	$\ddot{\xi}_{a3}$	$\bar{\ddot{\xi}}_{a1}$	$\bar{\ddot{\xi}}_{a2}$	$\bar{\ddot{\xi}}_{a3}$
0, 0, 0%												
2.5	250	48	42	7.5	4.5	5	7	6	8	2.6	3.6	6
2.0	115	57	35	5	6	5.5	6.5	7.8	9	1.8	6	7.8
1.5	200	50	18	9	7	3.6	5.5	10	12	4.9	10	7.5
1.0	55	18	50	4.5	4.5	15	7	14	46	3.1	8.5	4.8
0.5	40	9	8	5.7	4	4.5	9.5	17	28	9	17	28
2.5, 5, 5%												
2.5	150			5.8			6.8			2		
2.0	110			4.8			6			1.4		
1.5	95			4.8			5.8			2.3		
1.0	47			4			6.8			3		
0.5	24			3.8			8.5			5.8		
5, 5, 5%												
2.5	120	40	30	5	3.5	3.3	6.5	6	7	1.2	3	4.5
2.0	100	28	25	4.5	2.5	3.8	6	7	8.5	1.4	3	5.2
1.5	70	20	15	4	3	4	5.8	8	12.5	1.9	4.2	6
1.0	42	15	24	3.7	4	7.5	6.5	13	23	2.6	7	22
0.5	24	5.5	4.8	3.2	2.2	2.6	7.8	9.8	13	5	10	17

$r = 0.1936$ g's
$\ell = 10$ lines

T_1	x_{a1}	x_{a2}	x_{a3}	$\dot{x}_{a1}$	$\dot{x}_{a2}$	$\dot{x}_{a3}$	$\ddot{x}_{a1}$	$\ddot{x}_{a2}$	$\ddot{x}_{a3}$	$x_{a3}-x_{a2}$	$x_{a2}-x_{a1}$	$\dot{x}_{a3}-\dot{x}_{a2}$	$\dot{x}_{a2}-\dot{x}_{a1}$
0, 0, 0%													
2.5	290	240	260	8	8	8.3	3	2.4	2	250	140	9	6.4
2.0	110	130	150	6.5	5	7.2	3	3.2	3.5	130	100	8	8.5
1.5	200	180	190	9	9.6	12	6.5	5.8	5.4	190	120	10	9.5
1.0	60	65	70	6	6	9	7.2	10.2	9	90	57	13.5	10.5
0.5	40	38	40	6	6.8	8.5	13	13	11.5	42	26	8.5	7
2.5, 5, 5%													
2.5	140	140	150	5	5.5	8	2	2	1.5	160	85	5	4
2.0	100	100	100	5	4.1	5.6	2	2	1.8	110	60	5.2	4.9
1.5	90	95	100	4.5	5	5.2	3	2.9	2.8	90	55	5.5	4.1
1.0	45	48	45	3.8	4	5	3.5	4.	4.2	48	30	5.2	4.7
0.5	26	26	28	4	3.9	4.2	6.3	6.2	6	26	14	4	3.5
5, 5, 5%													
2.5	120	120	120	4.7	5	7.5	1.5	1.6	1.4	150	80	5	4
2.0	95	95	100	4.9	4	5.2	2	2	1.8	100	60	5.2	4.7
1.5	70	80	80	3	4.5	5	2.5	2.7	2.6	70	50	5.2	3.8
1.0	40	45	41	3.2	3.8	5	3	4	4.2	46	27	5	4.7
0.5	24	23	25	3.5	3.2	3.7	5.6	6	5.8	22	12	3.6	3.3

San Francisco
Taper

T_1	ξ_{a1}	ξ_{a2}	ξ_{a3}	$\dot{\xi}_{a1}$	$\dot{\xi}_{a2}$	$\dot{\xi}_{a3}$	$\ddot{\xi}_{a1}$	$\ddot{\xi}_{a2}$	$\ddot{\xi}_{a3}$	$\overline{\ddot{\xi}}_{a1}$	$\overline{\ddot{\xi}}_{a2}$	$\overline{\ddot{\xi}}_{a3}$
0, 0, 0%												
2.5	400	70	50	10	4	4.2	7.2	6.8	6.4	4.5	2.8	3.88
2.0	130	78	50	5	6.4	5.8	6	7.1	7.5	1.8	5.2	6.5
1.5	200	50	36	9.5	5	5.5	5.5	7.5	8	5	5.2	8
1.0	60	32	21	4.7	5.6	5.5	6.6	9	16	4	9	11.5
0.5	37	40	8.6	5.3	10	5	9	32	15	8	32	16
2.5, 5, 5%												
2.5	220			6.2			7			2		
2.0	90			4			6			1.5		
1.5	90			4.8			5.6			2.3		
1.0	53			4.1			6.3			3.1		
0.5	27			4			8			5.6		
5, 5, 5%												
2.5	180	50	38	5.5	.3	3.2	6.8	6.2	6	1.5	2	3
2.0	85	45	26	4.2	3.5	3.0	6	6.2	7	1.5	3	3.2
1.5	70	26	24	4.1	2.4	3.6	5.8	6.6	8	2.1	3.7	5
1.0	50	20	17	3.8	3.2	4.7	6	8	12.5	3	4.8	8
0.5	23	18	6.3	3.8	5.8	2.7	8	19	11	5	20	12

$r = 0.1936$ g's
$\ell = 10$ lines

T_1	x_{a1}	x_{a2}	x_{a3}	$\dot{x}_{a1}$	$\dot{x}_{a2}$	$\dot{x}_{a3}$	$\ddot{x}_{a1}$	$\ddot{x}_{a2}$	$\ddot{x}_{a3}$	$x_{a3}-x_{a2}$	$x_{a2}-x_{a1}$	$\dot{x}_{a3}-\dot{x}_{a2}$	$\dot{x}_{a2}-\dot{x}_{a1}$
0, 0, 0%													
2.5	400	380	380	10.5	11	12.5	4.2	5	2.3	360	210	11	7.5
2.0	160	130	170	7.5	6	10	4.2	3	3.2	150	140	8	9
1.5	200	200	220	11	10.5	12	7	6.5	4.9	200	130	12.5	9.6
1.0	70	65	85	7	6	8	7	6.5	5.8	75	57	7.6	7
0.5	45	40	50	8.2	6.4	10	20	13	13	38	37	7.8	10
2.5, 5, 5%													
2.5	200	200	200	6	6.5	8.2	2	2	1.3	200	90	5.6	4.8
2.0	85	90	110	4.5	4	6	2.6	2	1.5	80	75	4.7	4.2
1.5	88	90	95	6	5	5.8	3.2	3.9	2	90	43	5.5	5.7
1.0	54	50	56	4.8	4.1	5.2	4.1	4	2.8	47	35	4.7	3.8
0.5	28	28	35	5.8	4.5	6	11.5	9.5	8	26	22	4.8	6
5, 5, 5%													
2.5	150	150	150	5	5.5	7.5	1.6	1.8	1.2	160	80	5	4.2
2.0	80	85	100	4.2	4.5	6	2.4	1.5	1.4	80	70	5	4
1.5	75	70	70	5	4.4	5.1	3	2.4	1.7	80	40	5.2	5.2
1.0	48	47	50	4.4	4	5.2	3.8	3.8	2.3	42	32	4.2	3.6
0.5	24	25	30	5.2	4	5.2	10	9	7.2	22	20	4.5	5.8

San Francisco
Step

T_1	ξ_{a1}	ξ_{a2}	ξ_{a3}	$\dot{\xi}_{a1}$	$\dot{\xi}_{a2}$	$\dot{\xi}_{a3}$	$\ddot{\xi}_{a1}$	$\ddot{\xi}_{a2}$	$\ddot{\xi}_{a3}$	$\ddot{\bar{\xi}}_{a1}$	$\ddot{\bar{\xi}}_{a2}$	$\ddot{\bar{\xi}}_{a3}$
0, 0, 0%												
2.5	220	76	40	7	5	4	7	5.8	6.8	2.2	4	4.1
2.0	150	40	40	5.2	3.8	5.2	6	6.3	9	2.1	3	6
1.5	200	37	30	9	4	5	5	7.8	10.5	4.9	5	8
1.0	80	30	32	5.5	4.8	9	6	11.5	26	4.8	8	21
0.5	36	20	12.5	5.3	7.4	6.5	8	27	40	8.5	29	33
2.5, 5, 5%												
2.5	155			5.4			6.8			1.5		
2.0	140			4.7			6.2			1.5		
1.5	90			5			5			2.3		
1.0	52			4			6			3		
0.5	25			3.8			8.5			5.4		
5, 5, 5%												
2.5	120	50	27	5	3.5	2.6	6.6	6	6.5	1.2	2.6	2.7
2.0	125	33	27	4.1	2.8	3	6.2	6	7	1.4	2.6	4
1.5	80	25	15	4.4	2.8	3.2	5	6.5	10	2	3	4.6
1.0	48	14.5	20.5	3.5	3.1	6	6	10	18	2.8	4.4	14
0.5	20	12.6	5.7	3.3	4.5	3	8.5	16	14	4.8	15.5	15

$r = 0.1936$ g's
$\ell = 10$ lines

T_1	x_{a1}	x_{a2}	x_{a3}	$\dot{x}_{a1}$	$\dot{x}_{a2}$	$\dot{x}_{a3}$	$\ddot{x}_{a1}$	$\ddot{x}_{a2}$	$\ddot{x}_{a3}$	$x_{a3}-x_{a2}$	$x_{a2}-x_{a1}$	$\dot{x}_{a3}-\dot{x}_{a2}$	$\dot{x}_{a2}-\dot{x}_{a1}$
0, 0, 0%													
2.5	250	220	230	8	7.8	9	3.1	3	2.7	260	160	9.2	8
2.0	145	170	155	6	6	6.5	2.2	2.8	2.1	180	95	7.2	5.2
1.5	190	180	200	10	10	11	6.5	6	4.4	180	125	11	8.2
1.0	80	80	80	7	8	8.5	7	7.6	6.9	90	60	10.5	8
0.5	40	38	42	7	6.5	6.6	16.5	16	15.5	42	21	9	8
2.5, 5, 5%													
2.5	150	155	150	5	6	7.2	1.7	1.7	1.1	150	80	5	4.8
2.0	140	140	145	4.8	4.8	6	1.5	2	1.7	145	70	5.2	4
1.5	90	90	95	4.8	5.4	5.2	3	2.7	2.2	90	60	6.5	4.4
1.0	60	53	51	4.7	4.1	4.8	4.1	4	4.2	53	35	4.7	4.1
0.5	26	28	30	4.9	3.7	4.8	8	9.5	6.5	26	17	5.7	4.6
5, 5, 5%													
2.5	130	125	125	4.8	5.2	6.5	1.6	1.5	1.1	140	75	5	4.8
2.0	120	130	130	4.2	4	5.8	1.4	1.8	1.6	130	60	5	3.6
1.5	82	75	78	4.1	5	4.9	3	2.2	2.1	72	56	6	4.2
1.0	53	50	49	4	3.8	4.2	4.1	3.4	4	50	33	4.5	4
0.5	21	23	25	4.2	3	4.1	7.2	8.7	6.3	24	15	5.5	4.2

Taft
Uniform

T_1	ξ_{a1}	ξ_{a2}	ξ_{a3}	$\dot{\xi}_{a1}$	$\dot{\xi}_{a2}$	$\dot{\xi}_{a3}$	$\ddot{\xi}_{a1}$	$\ddot{\xi}_{a2}$	$\ddot{\xi}_{a3}$	$\overline{\ddot{\xi}}_{a1}$	$\overline{\ddot{\xi}}_{a2}$	$\overline{\ddot{\xi}}_{a3}$
0, 0, 0%												
2.5	340	420	330	7.5	32	38	7.2	30	50	4.4	30	49
2.0	460	450	230	18	40	30	11	48	42	7.8	46	47
1.5	220	72	105	15	11	30	12	15	52	8	14	52
1.0	90	100	14	10	25	5	9	60	15	6	60	16
0.5	150	25	4.5	26	10	2.5	42	47	16	45	53	19
2.5, 5, 5%												
2.5	320			6.8			7.2			4		
2.0	280			11.8			8.8			5.1		
1.5	180			10			12			7		
1.0	90			8.5			9			8		
0.5	80			12			21			20		
5, 5, 5%												
2.5	300	130	82	6.2	11.5	11.5	7	13.5	15	3.7	11.5	15.5
2.0	230	122	70	9.5	15.6	10.5	8	18.5	17.5	4	17	18
1.5	150	50	40	8	8	9	11	13	24	6	13	21
1.0	90	40	10	8	9.5	3	9	21	10	8	20	12
0.5	65	5.5	2.8	9.5	1.9	1.2	17.5	9	7.2	17	12	11.5

$r = 0.282$ g's
$\ell = 10$ lines

T_1	x_{a1}	x_{a2}	x_{a3}	$\dot{x}_{a1}$	$\dot{x}_{a2}$	$\dot{x}_{a3}$	$\ddot{x}_{a1}$	$\ddot{x}_{a2}$	$\ddot{x}_{a3}$	$x_{a3}-x_{a2}$	$x_{a2}-x_{a1}$	$\dot{x}_{a3}-\dot{x}_{a2}$	$\dot{x}_{a2}-\dot{x}_{a1}$
0, 0, 0%													
2.5	350	380	410	13.5	13	24	9.5	11.5	15.5	430	410	32	41
2.0	500	490	530	26	22	40	18	17	21	600	480	40	45
1.5	220	180	180	15	14	18	11	15	12	290	160	25	17
1.0	110	110	120	12	10.5	18	15	12	19	110	100	17	24
0.5	152	150	155	26	28	30	50	48	40	145	85	29	18
2.5, 5, 5%													
2.5	310	250	250	7	8	12.2	4.7	5.8	5.2	300	200	8.8	12
2.0	300	300	350	13.5	11.5	14	7.2	7.8	8.3	270	200	15	15.5
1.5	180	170	180	12	10	12	6.5	7.5	6	180	100	11	11
1.0	95	105	110	8.5	9.5	11	10.5	9	9	100	70	10	10
0.5	80	80	80	12	12	12	20	19.5	11	75	38	15	6.5
5, 5, 5%													
2.5	300	220	240	6.5	7.5	11.8	4.5	5.5	5.2	290	200	8.5	12
2.0	230	250	300	11	9.4	13	6.5	6.7	7.8	220	190	13	14.5
1.5	150	160	170	9	9	11	6	7	7	160	90	10	10.5
1.0	90	100	110	8	9	10.5	10	9	9.5	100	70	9	9.5
0.5	65	65	65	9.5	9.5	9.5	18	16.5	9	62	31	9.5	5.8

Taft
Taper

T_1	ξ_{a1}	ξ_{a2}	ξ_{a3}	$\dot{\xi}_{a1}$	$\dot{\xi}_{a2}$	$\dot{\xi}_{a3}$	$\ddot{\xi}_{a1}$	$\ddot{\xi}_{a2}$	$\ddot{\xi}_{a3}$	$\dddot{\xi}_{a1}$	$\dddot{\xi}_{a2}$	$\dddot{\xi}_{a3}$
0, 0, 0%												
2.5	340	250	200	7.8	20	22	7.1	15	21	4	13	19
2.0	410	170	160	18	16	20	10	15	27	7.5	13	24
1.5	250	320	135	12.5	36	22	10.5	42	39	7	42	38
1.0	130	100	80	9.5	16	19	10.5	30	50	9.8	41	50
0.5	150	14.5	9	27	5.5	4	45	19	18	45	18	20
2.5, 5, 5%												
2.5	320			6.5			7			4		
2.0	310			12.7			9			5.3		
1.5	170			9.5			10			5.5		
1.0	125			9			10.5			9		
0.5	80			12			20			19.5		
5, 5, 5%												
2.5	310	160	140	6.1	11	13	6.9	10	15	3.8	8.5	13.5
2.0	270	120	115	10.5	9.2	14	8.6	11.5	18	4.7	9.8	16.5
1.5	160	110	65	8	14	9.5	9.8	16.8	16.5	5.1	15	16
1.0	120	55	40	8	9	8.8	10	15.5	19.5	8.5	16	20
0.5	65	9.8	6	9.5	3	2.5	17	10.5	10.5	17	12.5	14

$r = 0.282$ g's
$\ell = 10$ lines

T_1	x_{a1}	x_{a2}	x_{a3}	$\dot{x}_{a1}$	$\dot{x}_{a2}$	$\dot{x}_{a3}$	$\ddot{x}_{a1}$	$\ddot{x}_{a2}$	$\ddot{x}_{a3}$	$x_{a3}-x_{a2}$	$x_{a2}-x_{a1}$	$\dot{x}_{a3}-\dot{x}_{a2}$	$\dot{x}_{a2}-\dot{x}_{a1}$
0, 0, 0%													
2.5	380	300	320	12.5	12	21	8.5	7	7.1	350	360	17	20
2.0	480	400	460	22	20	23	13	12	9	430	320	28	25
1.5	320	300	390	28	18	37	22	20	19	350	450	30	43
1.0	125	135	155	15	14.5	20	19	18	17.5	140	140	20	21
0.5	150	150	150	27	28	29	46	45	21	140	80	25	15
2.5, 5, 5%													
2.5	320	280	300	8.2	8	16	5.2	5	4.7	300	220	11.2	10.5
2.0	280	280	320	10	14.5	15.5	7	7	5.8	320	185	16.5	11
1.5	170	180	220	9	9.8	11	7.1	7	6	155	110	11.5	11.5
1.0	122	130	130	9.5	9	11	8.8	11.5	8	122	54	11.5	5
0.5	75	75	75	12.3	12	11	12	12	6	75	37	12	6.5
5, 5, 5%													
2.5	310	250	290	8	7.5	15	5.1	5	4.7	290	210	10.8	10.5
2.0	230	230	270	8.5	11.5	14.5	5.5	6.6	5.8	300	140	14	10
1.5	150	165	190	8.8	8.2	11.8	7	6.3	5.8	140	100	10	11.5
1.0	115	122	122	8.5	8.3	10.5	8.8	11	7	115	50	11	4.7
0.5	62	63	65	10	9.5	9	9.8	9.6	4.8	60	30	10	5.5

Taft Step T_1	ξ_{a1}	ξ_{a2}	ξ_{a3}	$\dot{\xi}_{a1}$	$\dot{\xi}_{a2}$	$\dot{\xi}_{a3}$	$\ddot{\xi}_{a1}$	$\ddot{\xi}_{a2}$	$\ddot{\xi}_{a3}$	$\dddot{\xi}_{a1}$	$\dddot{\xi}_{a2}$	$\dddot{\xi}_{a3}$
0, 0, 0%												
2.5	330	220	500	7.3	18.5	42	7.2	17	49	4	15	50
2.0	450	300	220	18	23	25	11	23	32	8.4	22	36
1.5	270	165	85	17.5	21	15	11	30	28	7.2	30	30
1.0	126	95	41	10	18	11.5	10.5	40	35	10.5	38	35
0.5	160	27	6.6	28	8.5	3.6	47	32	19	48	37	20
2.5, 5, 5%												
2.5	320			6.6			7.2			3.9		
2.0	300			12.2			8.8			5.5		
1.5	175			9.5			10.2			6		
1.0	130			9.2			10			9.5		
0.5	80			12.6			21			21		
5, 5, 5%												
2.5	300	135	125	6.2	9	15	7	9.6	17	3.8	9.5	16.5
2.0	240	140	66	10.5	12.5	8.5	8	15	13	4.3	13	13.5
1.5	160	85	48	8.5	10.2	8	10	13.5	15	5.5	14	16
1.0	122	48	18	8	8.8	4	9.6	16	10.5	9	17	15
0.5	68	8	4	10	2.6	1.5	18	9	8	18	12	11.7

r = 0.282 g's

ℓ = 10 lines

T_1	x_{a1}	x_{a2}	x_{a3}	$\dot{x}_{a1}$	$\dot{x}_{a2}$	$\dot{x}_{a3}$	$\ddot{x}_{a1}$	$\ddot{x}_{a2}$	$\ddot{x}_{a3}$	$x_{a3}-x_{a2}$	$x_{a2}-x_{a1}$	$\dot{x}_{a3}-\dot{x}_{a2}$	$\dot{x}_{a2}-\dot{x}_{a1}$
0, 0, 0%													
2.5	300	340	360	15	14.5	24	10	12	12	450	400	40	30
2.0	520	510	510	27	22	30	15.5	16.5	13	520	420	36	34
1.5	300	230	280	16	15.5	19	15	12.5	12	280	250	19.5	22
1.0	125	135	130	12	11	15	15	14	14	130	110	16.5	18.5
0.5	165	162	170	32	28	30	55	50	40	150	100	30	22
2.5, 5, 5%													
2.5	280	300	320	6.2	7.5	11	3.8	5	5	300	170	12.5	10
2.0	270	320	320	12.5	14	12	7	8.5	5.5	300	200	16	14
1.5	190	180	200	10	9.8	11.3	8.2	7.5	7.1	180	130	11.5	11
1.0	130	125	125	10.5	9	10	9.2	11.5	8.2	130	65	9	9
0.5	82	82	83	13	13	13	22	22	13	77	45	12	7
5, 5, 5%													
2.5	250	270	300	6	7.3	11	3.7	4.7	4.7	300	160	12.6	10
2.0	230	260	200	9.8	11.5	11	6.5	7.3	5.5	250	180	14	12.5
1.5	160	170	185	9	8.5	10	7.5	7	6.8	160	115	10.5	10
1.0	120	115	120	9.6	8	9.8	8.8	11	7.5	120	60	8.5	8
0.5	68	68	70	10.5	10	10	20	18	11	65	38	10	6

El Centro
Uniform

T_1	ξ_{a1}	ξ_{a2}	ξ_{a3}	$\dot{\xi}_{a1}$	$\dot{\xi}_{a2}$	$\dot{\xi}_{a3}$	$\ddot{\xi}_{a1}$	$\ddot{\xi}_{a2}$	$\ddot{\xi}_{a3}$	$\dddot{\xi}_{a1}$	$\dddot{\xi}_{a2}$	$\dddot{\xi}_{a3}$
0, 0, 0%												
2.5	380	170	110	16	20	19	10.5	25	32	6.6	23	30
2.0	410	130	105	23	19	22	14	30	50	11.5	27	50
1.5	190	95	98	14.5	18	28	12	38	70	9.5	40	80
1.0	155	40	42	17	9.5	18	23	30	80	17	30	90
0.5	160	20	5	40	13	4	75	73	30	75	75	40
2.5, 5, 5%												
2.5	300			14			7.2			5		
2.0	300			17.5			11.8			8.5		
1.5	110			8			8			5		
1.0	90			10			11			9.5		
0.5	60			12			26			27		
5, 5, 5%												
2.5	270	80	60	13	9.3	10.5	7	11.5	17.5	4.5	10.5	16
2.0	240	58	41	14	8	9.5	10	12.5	19	6.7	12	18
1.5	80	55	21	7	11	6	8	19	14.5	4.5	18	17
1.0	80	18	10	8.5	5	4.5	10	14	17.5	8	16.	17
0.5	50	4.2	1.3	10.5	1.9	0.8	20	11	6	19	13.5	9

$r = 0.35$ g's
$\ell = 10$ lines

T_1	x_{a1}	x_{a2}	x_{a3}	$\dot{x}_{a1}$	$\dot{x}_{a2}$	$\dot{x}_{a3}$	$\ddot{x}_{a1}$	$\ddot{x}_{a2}$	$\ddot{x}_{a3}$	$x_{a3}-x_{a2}$	$x_{a2}-x_{a1}$	$\dot{x}_{a3}-\dot{x}_{a2}$	$\dot{x}_{a2}-\dot{x}_{a1}$
0, 0, 0%													
2.5	420	400	420	16	18	25	10.5	11	12.5	410	300	26	28
2.0	420	440	480	28	23	28	14.5	17	16.5	450	280	32	32
1.5	220	190	240	18	19	30	21	20	24	280	210	30	28
1.0	155	160	160	18	17	19	18	26	19	140	90	23	18.5
0.5	170	170	170	40	38	45	90	80	60	160	100	40	30
2.5, 5, 5%													
2.5	310	300	300	14	15	15.5	6.8	5.5	6.5	300	200	14	13.5
2.0	300	310	330	18	15.5	15.5	8.5	10.5	8	300	150	18.5	14.5
1.5	110	140	100	9	11	11	14.5	7	9	100	100	7.5	8.5
1.0	90	85	85	10.5	9	8.5	9	11	8	80	85	10	11
0.5	60	60	60	12	12	12	16	25	23	55	30	12	6.8
5, 5, 5%													
2.5	280	260	290	13	14	14.5	6.2	5	6.1	270	180	13	13.5
2.0	230	260	270	15.5	12.2	12	7.2	9	7.1	220	130	16	13
1.5	100	85	80	7	7	6.5	14	6	8	85	85	6.5	7
1.0	80	80	77	9	8	8	8.5	10	7.5	70	80	9	10
0.5	50	50	48	10.5	10.5	10.5	13.5	18	19	45	24	10.5	5.5

El Centro
Taper

T_1	ξ_{a1}	ξ_{a2}	ξ_{a3}	$\dot{\xi}_{a1}$	$\dot{\xi}_{a2}$	$\dot{\xi}_{a3}$	$\ddot{\xi}_{a1}$	$\ddot{\xi}_{a2}$	$\ddot{\xi}_{a3}$	$\bar{\ddot{\xi}}_{a1}$	$\bar{\ddot{\xi}}_{a2}$	$\bar{\ddot{\xi}}_{a3}$
0, 0, 0%												
2.5	400	400	200	16.5	44	28	11	30	32	6.8	29	32
2.0	430	110	165	24	12	28	14.5	13	40	12	13	41
1.5	200	130	190	15	19	41	12	33	82	10	27	82
1.0	155	90	50	18	19	14.5	22	45	45	16	42	41
0.5	155	34	8.5	35	13.5	5	70	57	30	70	61	35
2.5, 5, 5%												
2.5	300			15			7.8			5.4		
2.0	310			18			12			8.8		
1.5	110			8.5			8.5			6		
1.0	94			10.5			11.5			10		
0.5	62			12			25			26		
5, 5, 5%												
2.5	280	150	85	14	14	10.5	7.2	14	12	4.7	11	12
2.0	260	78	60	14	8.6	8.7	10.5	10.5	15	7	9	13
1.5	95	60	50	7.8	8.2	11	7.6	12.5	20	5	11	19.5
1.0	86	40	14.5	9	9	3.8	11	19	11	9.5	18	13
0.5	48	8	3	10	3.2	1.4	20	14	7.6	19	14.5	10.5

$r = 0.35$ g's
$\ell = 10$ lines

T_1	x_{a1}	x_{a2}	x_{a3}	$\dot{x}_{a1}$	$\dot{x}_{a2}$	$\dot{x}_{a3}$	$\ddot{x}_{a1}$	$\ddot{x}_{a2}$	$\ddot{x}_{a3}$	$x_{a3}-x_{a2}$	$x_{a2}-x_{a1}$	$\dot{x}_{a3}-\dot{x}_{a2}$	$\dot{x}_{a2}-\dot{x}_{a1}$
0, 0, 0%													
2.5	530	420	630	28	26	35	16.5	15	15	480	480	34	40
2.0	500	420	500	27	30	29	16.5	17.5	13.5	420	310	35	30
1.5	260	270	280	22	21	30	26	30	22	330	220	38	40
1.0	170	163	180	22	23	33	32	28	25	180	140	27	28
0.5	170	150	160	40	35	40	90	75	55	150	95	35	36
2.5, 5, 5%													
2.5	300	320	340	15	15.5	17.5	7.5	7.5	6.5	330	190	15.3	14
2.0	280	300	370	16	19	18	12.5	9.5	8.5	300	220	22	14
1.5	125	120	127	10	9	11.5	8	9	6.5	120	80	11.3	9.6
1.0	100	96	100	10.1	11.5	11.8	11	12	10	90	59	10.8	9.2
0.5	58	52	60	12	12.2	12.5	27	26	14.5	53	34	12	8
5, 5, 5%													
2.5	280	280	300	12.5	14.5	16.8	7.2	7	6.5	300	180	14	13
2.0	280	280	300	14	16	15	11	8	7.5	240	200	19	13
1.5	113	105	108	8	8	9.5	8	7	6	100	75	11	9.5
1.0	90	90	94	9.8	10.4	10.6	11.5	10.5	9.5	82	55	9.6	9
0.5	48	47	49	10.5	10.5	10.4	21	19	12.5	45	27	10	7.8

El Centro
Step

T_1	ξ_{a1}	ξ_{a2}	ξ_{a3}	$\dot{\xi}_{a1}$	$\dot{\xi}_{a2}$	$\dot{\xi}_{a3}$	$\ddot{\xi}_{a1}$	$\ddot{\xi}_{a2}$	$\ddot{\xi}_{a3}$	$\ddot{\bar{\xi}}_{a1}$	$\ddot{\bar{\xi}}_{a2}$	$\ddot{\bar{\xi}}_{a3}$
0, 0, 0%												
2.5	400	165	80	17	16	10.8	11	18.5	16	6.8	15.5	14.5
2.0	450	190	300	24	26	51	15	31	90	11.8	30	87
1.5	200	140	70	15.5	25	16	13	40	37	10.5	39	35
1.0	155	98	50	17	24	21	23	58	71	16	55	70
0.5	155	12	4.8	35	52	28	70	25	17	70	29	20
2.5, 5, 5%												
2.5	320			15			8			5.7		
2.0	340			18			12.3			9		
1.5	110			8.6			8.3			5.6		
1.0	105			11			12			11		
0.5	60			12			25			25		
5, 5, 5%												
2.5	300	102	60	14	9.6	8.5	7.6	12	12	5	9.8	11.2
2.0	280	78	63	14.5	10	11.5	11	11.8	19	7.2	11.5	18
1.5	95	54	33	7.8	9	7.5	7.7	16	18	5	13.5	16.8
1.0	94	30	13.2	10	7.3	4.5	11.4	17.5	13	10	16	15.6
0.5	52	6	1.9	10	24	11.5	20	12	6.7	19	13	9.8

$r = 0.35$ g's
$\ell = 10$ lines

T_1	x_{a1}	x_{a2}	x_{a3}	$\dot{x}_{a1}$	$\dot{x}_{a2}$	$\dot{x}_{a3}$	$\overline{\ddot{x}}_{a1}$	$\overline{\ddot{x}}_{a2}$	$\overline{\ddot{x}}_{a3}$	$x_{a3}-x_{a2}$	$x_{a2}-x_{a1}$	$\dot{x}_{a3}-\dot{x}_{a2}$	$\dot{x}_{a2}-\dot{x}_{a1}$
0, 0, 0%													
2.5	430	390	450	19	18	22	11.5	8.5	8.2	420	340	21	21
2.0	480	490	500	30	30	38	25	23	24	530	420	47	45
1.5	260	240	270	21	20	23	19	17.5	15	230	220	28	27
1.0	170	170	210	22	19.5	30	33	30	31	210	155	40	33
0.5	155	150	160	35	34	40	73	71	48	145	90	40	20
2.5, 5, 5%													
2.5	330	320	320	14	16.5	15	7.7	6.2	5.5	300	220	17.2	12
2.0	330	370	380	20	19	18	11.5	11	10.2	350	200	22	18
1.5	110	110	115	9.8	9	10.3	6.7	7	6	110	70	10.6	9.6
1.0	103	105	110	11	11.6	11.3	13	12	9	95	63	12	8.5
0.5	57	58	59	12	12	12	27	24	15.5	55	30	11.8	7.6
5, 5, 5%													
2.5	290	270	280	13	15.5	14	7	5.8	5.4	270	210	16	12.5
2.0	280	290	300	16	15.5	14	9.7	9	9	270	160	18	16.5
1.5	100	105	105	8.4	8.1	9	7	6.1	5.3	94	70	9.7	10
1.0	89	100	100	9.8	10	10	11	11	8.3	83	55	10.5	8
0.5	49	50	49	10.5	10.5	10.2	21	19	13	47	26	10.2	7.2